

Effects of the Heterocycle and Its Substituents on Structure and Fluxionality in Rhodium(I) and Iridium(I) Complexes with the Hindered Thiolates 6-*tert*-Butylpyridine-2-thiolate and 1-Alkyl-4-*tert*-butylimidazole-2-thiolate (alkyl = methyl and *tert*-butyl)

Valentín Miranda-Soto,[‡] Jesús J. Pérez-Torrente,[†] Luis A. Oro,[†] Fernando J. Lahoz,[†] M. Luisa Martín,[†] Miguel Parra-Hake,[‡] and Douglas B. Grotjahn^{*,†,§}

Centro de Graduados e Investigación, Instituto Tecnológico de Tijuana, Apartado Postal 1166, 22000 Tijuana, Baja California, México, and Departamento de Química Inorgánica, Instituto Universitario de Catálisis Homogénea, Instituto de Ciencia de Materiales de Aragón, Universidad de Zaragoza-Consejo Superior de Investigaciones Científicas, 50009 Zaragoza, Spain, and Department of Chemistry and Biochemistry, San Diego State University, 5500 Campanile Drive, San Diego, California 92182-1030

Received April 9, 2006

Three new sterically hindered heterocyclic thiolate ligands are studied (HetS = 6-*tert*-butylpyridine-2-thiolate, ^tBu-PyS; 1-methyl-4-*tert*-butylimidazole-2-thiolate, Me-^tBu-ImS; 1,4-di-*tert*-butylimidazole-2-thiolate, ^tBu₂-ImS). Related Rh(I) and Ir(I) metal complexes with molecular formulas [M(HetS)(COD)]_n, [M(HetS)(CO)₂]_n, and [M(HetS)(CO)(PPh₃)_n] (where *n* = 1 or 2) were made to assess the steric and electronic effects of heterocycle (pyridine vs imidazole) and bulky substituents on the ring. A combination of solution-phase molecular weight determination, infrared spectroscopy, variable-temperature NMR, and solid-state X-ray diffraction studies were used to determine the molecularity of the complexes (value of *n*) and the coordination modes of the ligands. In the pyridine series, no evidence was found for nitrogen coordination; the presence of the *tert*-butyl group makes the heterocyclic thiolate behave like a nonheterocyclic derivative. In the imidazole series, three coordination modes were found, all of them including complexation through both the thiolate sulfur and the basic ring nitrogen. Evidence for fluxional and dimer–monomer interconversions was found for several of the imidazole derivatives, and the size of the 1-alkyl group played a significant role in determining the structures of the complexes.

Introduction

In the evolution of organometallic chemistry, phosphines rapidly became a privileged class of ligands because one can modulate the structure and reactivity of metal complexes and their reactivity through extensive electronic and steric variation of all three phosphorus substituents.^{1,2} In comparison, thiolate ligands³ are less utilized, although they are of particular interest for their roles in metalloenzymes, metallopharmaceuticals, and other areas.⁴ Thiolates show a strong tendency to form bridging polynuclear species, control of which can be achieved in some measure by use of steric or electronic factors. Heterocyclic thiolates present an interesting and useful subclass, because the heterocyclic nitrogen is an additional site for coordination.⁵ Taken together, common coordination modes for heterocyclic

thiolates include not only those displayed by nonheterocyclic thiolates (e.g., **B** in Chart 1) but also head-to-head and head-to-tail bridging (e.g., **D** and **E**). Less common coordination modes are mixed forms such as **C**, and in mononuclear species (**A**) as a chelating ligand.

Part of our interest in heterocyclic thiolates stems from results using related phosphines in bifunctional catalysis.⁶ Heterocyclic phosphines are responsible for dramatic enhancements in catalysis of alkyne anti-Markovnikov hydration,⁷ alkyne alkoxy-carbonylation,⁸ nitrile hydration,⁹ and certain H/D exchange reactions.¹⁰ Various roles have been discussed for these bifunctional ligands. Recent structural and stoichiometric reactivity studies by the Grotjahn group on pyrid-2-yl and imidazol-

* Corresponding author. E-mail: grotjahn@chemistry.sdsu.edu.

[‡] Instituto Tecnológico de Tijuana.

[†] Universidad de Zaragoza-CSIC.

[§] San Diego State University.

(1) Collman, J. P.; Hegedus, L. S.; Norton, J. R.; Finke, R. G. *Principles and Applications of Organotransition Metal Chemistry*; University Science Books: Mill Valley, CA, 1987.

(2) Crabtree, R. H. *The Organometallic Chemistry of the Transition Metals*, 3rd ed.; Wiley: New York, 2000.

(3) (a) Dance, I. G. *Polyhedron* **1986**, *5*, 1037. (b) Dilworth, J. R.; Hu, J. *Adv. Inorg. Chem.* **1994**, *40*, 411.

(4) Examples: (a) Mascharak, P. K. *Coord. Chem. Rev.* **2002**, *225*, 201. (b) Kovacs, J. A. *Chem. Rev.* **2004**, *104*, 825. (c) Holm, R. H.; Kennepohl, P.; Solomon, E. I. *Chem. Rev.* **1996**, *96*, 2239. (d) Hille, R. *Chem. Rev.* **1996**, *96*, 2757. (e) Howard-Lock, H. E. *Metal-Based Drugs* **1999**, *6*, 201. (f) Tieckink, E. R. T. *Bioinorg. Chem. Appl.* **2003**, *1*, 53.

(5) (a) Akrivos, P. D. *Coord. Chem. Rev.* **2001**, *213*, 181. (b) Raper, E. S. *Coord. Chem. Rev.* **1997**, *165*, 475. (c) Raper, E. S. *Coord. Chem. Rev.* **1996**, *153*, 199. (d) Sadimenko, A. P. *Adv. Heterocycl. Chem.* **2003**, *84*, 191. (e) Garnovskii, A. D.; Sadimenko, A. P.; Sadimenko, M. I.; Garnovskii, D. A. *Coord. Chem. Rev.* **1998**, *173*, 31.

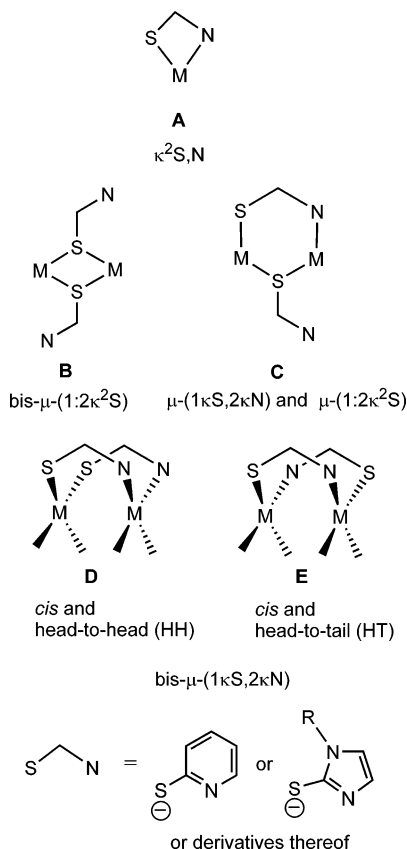
(6) Grotjahn, D. B. *Chem. Eur. J.* **2005**, *11*, 7146. (7) (a) Grotjahn, D. B.; Incarvito, C. D.; Rheingold, A. L. *Angew. Chem., Int. Ed.* **2001**, *40*, 3884. (b) Grotjahn, D. B.; Lev, D. A. *J. Am. Chem. Soc.* **2004**, *126*, 12232. (c) Lev, D. A.; Grotjahn, D. B. *Catal. Org. React.* **2005**, *104*, 237. (d) Grotjahn, D. B.; Lev, D. A. *Catal. Org. React.* **2005**, *104*, 227.

(8) (a) Drent, E.; Arnoldy, P.; Budzelaar, P. H. M. *J. Organomet. Chem.* **1993**, *455*, 247. (b) Drent, E.; Arnoldy, P.; Budzelaar, P. H. M. *J. Organomet. Chem.* **1994**, *475*, 57.

(9) Oshiki, T.; Yamashita, H.; Sawada, K.; Utsunomiya, M.; Takahashi, K.; Takai, K. *Organometallics* **2005**, *24*, 6287.

(10) Jalon, F. A.; Manzano, B. R.; Caballero, A.; Carrion, M. C.; Santos, L.; Espino, G.; Moreno, M. *J. Am. Chem. Soc.* **2005**, *127*, 15364.

Chart 1. Relevant Coordination Modes of Pyridine- and Imidazole-2-thiolates



2-yl phosphines have begun to show intriguing differences between the two heterocyclic substituents¹¹ as well as the role of not only the imidazole but also the phosphorus substituents on the propensity for forming monodentate κ^1 -P or chelating κ^2 -P,N species.¹² In the work presented here, one larger goal is to examine similar factors in heterocyclic thiolate complexes, because the sulfur atom bears only the heterocycle and not two additional groups. Hence, one might be able to focus solely on the steric and electronic contribution of the heterocycle and its substituents.

Coordination of pyridine-2-thiolate (PyS) to Rh(I) and Ir(I) species as in $M_2(PyS)_2L^1L^2$, where L^1 and L^2 are CO, alkenes, or CO and phosphine, has established that doubly bridged species of types **C** and **E** could be formed and may interconvert in solution.¹³ The closely related species 1-alkylimidazole-2-thiolate has to our knowledge not been examined on Rh(I) or Ir(I), although it has shown a variety of coordination modes in other systems.^{14–17} In the work reported here, we chose to increase steric hindrance at the basic heterocyclic nitrogen by using derivatives with an adjacent *tert*-butyl group. In addition,

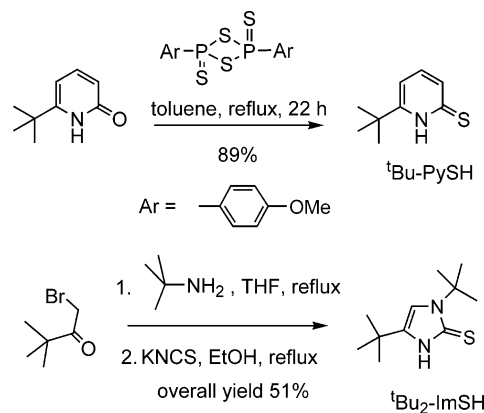
(11) Grotjahn, D. B.; Hoerter, J. M.; Lev, D. A.; Dwyer, T. J. Unpublished results.

(12) Grotjahn, D. B.; Gong, Y.; Zakharov, L. N.; Golen, J. A.; Rheingold, A. L. *J. Am. Chem. Soc.* **2006**, *128*, 438.

(13) (a) Oro, L. A.; Ciriano, M. A.; Pérez-Torrente, J. J.; Villarroja, B. E. *Coord. Chem. Rev.* **1999**, *1*. (b) Ciriano, M. A.; Viguri, F.; Pérez-Torrente, J. J.; Lahoz, F. J.; Oro, L. A.; Tiripicchio, A.; Tiripicchio-Camellini, M. *J. Chem. Soc., Dalton Trans.* **1989**, 25. (c) Dahlenburg, L. Kühnlein, M. *Eur. J. Inorg. Chem.* **2000**, 2117. (d) Oro, L. A.; Ciriano, M. A.; Viguri, F.; Tiripicchio, A.; Tiripicchio-Camellini, M.; Lahoz, F. J. *Nouv. J. Chim.* **1986**, *10*, 75.

(14) (a) Azam, K. A.; Hanif, K. M.; Ghosh, A. C.; Kabier, S. E.; Karmakar, S. R.; Malik, K. M. A.; Parvin, S.; Rosemberg, E. *Polyhedron* **2002**, *21*, 885. (b) Bonati, F.; Burini, A.; Pietroni, B. R.; Giorgini, E.; Bovio, B. *J. Organomet. Chem.* **1988**, *344*, 119.

Scheme 1. Syntheses of New Thioles



studying the effect of the steric environment of the thiolate sulfur was accomplished in the imidazole series by making 1-methyl and 1-*tert*-butyl derivatives.

Results

Ligand Synthesis. 6-*tert*-Butylpyridine-2-one is a known compound¹⁸ that could be readily converted to the novel thio analogue 6-*tert*-butylpyridine-2-thiol (^tBu-PySH) using Lawesson's reagent (Scheme 1). In the imidazole series, the 1,4-di-*tert*-butyl derivative was new, made as had been recently the 1-methyl-4-*tert*-butyl analogue¹⁹ using a method patterned after that for the 1-isopropyl-4-*tert*-butyl analogue.²⁰

Complexes Derived from 6-*tert*-Butylpyridine-2-thiol (^tBu-PySH). The direct protonation of the methoxide bridging ligands in the complexes $[M(\mu\text{-OMe})(\text{COD})]_2$ ($M = \text{Rh}, \text{Ir}$) by 6-*tert*-butylpyridine-2-thiol (^tBu-PySH) in dichloromethane resulted in the formation of the dinuclear complexes $[\text{Rh}(\mu\text{-}^t\text{Bu-PyS})(\text{COD})]_2$ (**1**, Scheme 2) and $[\text{Ir}(\mu\text{-}^t\text{Bu-PyS})(\text{COD})]_2$ (**2**), which were isolated as yellow and red microcrystalline solids in good yield. The determination of the molecular weight in chloroform supports the dinuclear formulation of the complexes. In addition, the FAB+ spectra showed the dinuclear ions at m/z 755 and 933, respectively.

The ¹H NMR spectrum of compound **1** in CD₂Cl₂ at RT showed three resonances at δ 7.38 (t), 7.16 (d), and 7.04 (d), for the aromatic protons of the equivalent 6-*tert*-butylpyridine-2-thiolate (^tBu-PyS⁻) ligands, and a singlet at δ 1.32 ppm for the ^tBu groups. The diolefin region of the spectrum showed broad resonances and evidenced a fluxional behavior on the NMR time scale. Thus, at 25 °C, the =CH and >CH₂ protons

(15) (a) Shu, M.; Walz, R.; Wu, B.; Seebacher, J.; Vahrenkamp, H. *Eur. J. Inorg. Chem.* **2003**, 2502. (b) Bell, N. A.; Clegg, W.; Creighton, J. R.; Raper, E. S. *Inorg. Chim. Acta* **2000**, *303*, 12. (c) Ruiz, J.; Florenciano, G.; López, G.; Chaloner, P. A.; Hitchcock, P. B. *Inorg. Chim. Acta* **1998**, *281*, 165. (d) Yap, G. P. A.; Jensen, C. M. *Inorg. Chem.* **1992**, *31*, 4823. (e) Wilton-Ely, J. D. E. T.; Honarkah, S. J.; Wang, M.; Tocher, D. A.; Slawin, A. M. Z. *Dalton Trans.* **2005**, 1930.

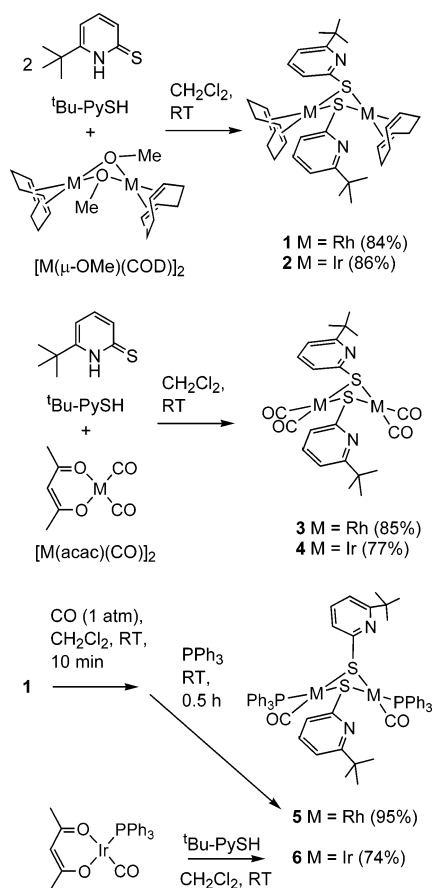
(16) (a) Allan, R. A.; Bashall, A.; Palmer, J. S.; McPartlin, M.; Mosquera, M. E. G.; Rawson, J. M.; Weatherly, A. E. H.; Wright, D. S. *Chem. Commun.* **1997**, 1975. (b) Raper, E. S.; Creighton, J. R.; Clegg, W. *Inorg. Chim. Acta* **1991**, *183*, 179. (c) Cooper, D. A.; Rettig, S. J.; Storr, A.; Trotter, J. *Can. J. Chem.* **1986**, *64*, 1643.

(17) (a) Brandt, K.; Sheldrick, W. S. *Inorg. Chim. Acta* **1998**, *267*, 39. (b) Landgrabe, C.; Sheldrick, W. S.; Sudfeld, M. *Eur. J. Inorg. Chem.* **1998**, 407. (c) Lowe, G.; Ross, S. A.; Probert, M.; Cowley, A. *Chem. Commun.* **2001**, 1288.

(18) Baur, J.; Jacobsen, H.; Burger, P.; Artus, G.; Berke, H.; Dahlenburg, L. *Eur. J. Inorg. Chem.* **2000**, 1411.

(19) Miranda-Soto, V.; Parra-Hake, M.; Morales-Morales, D.; Toscano, R. A.; Boldt, G.; Koch, A.; Grotjahn, D. B. *Organometallics* **2005**, *24*, 5569.

(20) Corey, E. J.; Brunelle, D. J. *Tetrahedron Lett.* **1976**, 3409.

Scheme 2. Syntheses of ^tBu-PyS Complexes

were observed as one resonance at δ 4.84 ppm and two resonances at δ 2.42 and 1.96 ppm, respectively. However, on cooling at -70 °C the =CH protons were observed as two resonances at δ 4.98 and 4.43 ppm. This dynamic behavior can also be detected in the $^{13}\text{C}\{^1\text{H}\}$ NMR spectrum, where the =CH carbons were observed as two broad resonances at δ 81.3 and 77.9 ppm at -70 °C and as a doublet at δ 80.3 ppm ($J_{\text{Rh-C}} = 11.9$ Hz) at room temperature. The spectroscopic information obtained from the variable-temperature NMR analysis suggests an open-book structure resulting from the thiolate μ -(1:2 κ^2 S) coordination mode of both ^tBu-PyS[−] ligands with a *syn* disposition. In fact, the inversion of the nonplanar Rh₂S₂ ring^{21,22a–d} would account for the equivalence of all the olefinic =CH protons and carbons at room temperature.

The behavior in solution of compound $[\text{Ir}(\mu\text{-}^t\text{Bu-PyS})(\text{COD})]_2$ (**2**) is identical to that of compound **1**, which strongly supports a similar structure with a C_{2v} symmetry. In particular, the ¹H NMR spectrum in CDCl₃ at -55 °C showed the expected two broad resonances for the =CH protons and four sharp multiplets for the >CH₂ protons as a consequence of the differentiation between the two groups of *exo* and *endo* protons.²³ The molecular structure of **2** was determined by an X-ray diffraction analysis (discussed below) and is shown in Figure 1. The

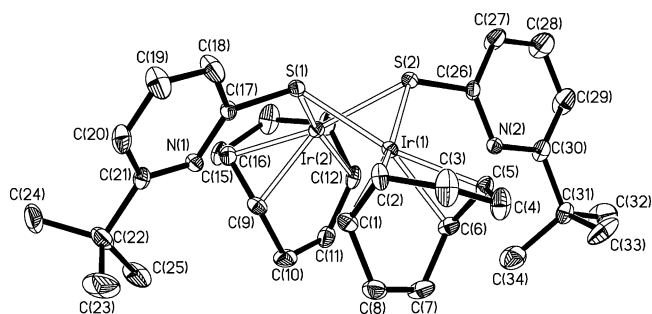


Figure 1. Molecular structure of compound $[\text{Ir}(\mu\text{-}^t\text{Bu-PyS})(\text{COD})]_2$ (**2**).

structure confirms the thiolate coordination μ -(1:2 κ^2 S) of the 6-*tert*-butylpyridine-2-thiolate ligands that adopt a relative *syn-endo* disposition.

The reaction of the mononuclear complexes $[\text{M}(\text{acac})(\text{CO})]_2$ (M = Rh, Ir) with 6-*tert*-butylpyridine-2-thiol (^tBu-PySH) in dichloromethane (1:1 molar ratio) gave deeply colored solutions from which the dinuclear compounds $[\text{Rh}(\mu\text{-}^t\text{Bu-PyS})(\text{CO})_2]_2$ (**3**, Scheme 2) and $[\text{Ir}(\mu\text{-}^t\text{Bu-PyS})(\text{CO})_2]_2$ (**4**) were isolated as red and green microcrystalline solids, respectively, in good yield. It is noticeable that solutions of compounds **3** and **4** can also be prepared by direct carbonylation of compounds **1** and **2** in dichloromethane. However, the presence of free 1,5-cyclooctadiene in the reaction media makes the isolation of the complexes difficult.

The dinuclear formulation of the complexes relies on the FAB⁺ spectra, which showed the molecular ions at *m/z* 650 and 829 and the sequential losses of several carbonyl ligands. Moreover, the IR spectra indicate that the coordination mode of the bridging ^tBu-PyS[−] ligands (1:2 κ^2 S) remains unchanged upon carbonylation. Thus, the IR spectra of both compounds in dichloromethane showed three $\nu(\text{CO})$ bands for the terminal carbonyl groups at 2082 (m), 2064 (s), and 2016 (s) cm^{-1} (compound **3**) and 2073 (m), 2053 (s), and 2002 (s) cm^{-1} (compound **4**). This pattern of intensities (m, s, s) is typical for tetracarbonyl dinuclear complexes having thiolato ligands as bridges²⁴ and is distinct from that seen for *cis*-HT dimers of type **E**.¹³

The ¹H NMR spectra at RT of both complexes showed equivalent ^tBu-PyS[−] ligands. The only observed temperature effect was the slight broadening of the resonances for both complexes at -50 °C in CDCl₃. The equivalent carbonyl ligands were observed as a doublet at δ 184.4 ppm ($J_{\text{Rh-C}} = 71.9$ Hz) and a singlet at δ 173.4 ppm in the $^{13}\text{C}\{^1\text{H}\}$ NMR spectra of **3** and **4**, respectively, in agreement with a C_{2v} symmetry structure resulting from a *syn* disposition of the bridging thiolato ligands (Scheme 2).

The tetracarbonyl compound $[\text{Rh}(\mu\text{-}^t\text{Bu-PyS})(\text{CO})_2]_2$ (**3**), obtained in situ by carbonylation of diolefin complex $[\text{Rh}(\mu\text{-}^t\text{Bu-PyS})(\text{COD})]_2$ (**1**) in dichloromethane, was reacted with 2 molar equiv of triphenylphosphine to give the complex $[\text{Rh}(\mu\text{-}^t\text{Bu-PyS})(\text{CO})(\text{PPh}_3)]_2$ (**5**, Scheme 2) after evolution of carbon monoxide. However, the related iridium complex $[\text{Ir}(\mu\text{-}^t\text{Bu-PyS})(\text{CO})(\text{PPh}_3)]_2$ (**6**) was better obtained from the reaction of $[\text{Ir}(\text{acac})(\text{CO})(\text{PPh}_3)]$ with ^tBu-PySH in dichloromethane. Compound **5** was isolated as a moderately stable yellow solid, but

(21) Abel, E. W.; Orrell, K. G. *Prog. Inorg. Chem.* **1984**, 32, 1.

(22) (a) Brunner, H.; Bügler, J.; Nuber, B. *Tetrahedron Asymmetry* **1996**, 7, 3095. (b) Fernández, E.; Ruiz, A.; Castellón, S.; Claver, C.; Piniella, J. F.; Alvarez-Larena, A.; Germani, G. *J. Chem. Soc., Dalton Trans.* **1995**, 2137. (c) Ciriano, M. A.; Pérez-Torrente, J. J.; Lahoz, F. J.; Oro, L. A. *J. Chem. Soc., Dalton Trans.* **1992**, 1831. (d) Cotton, F. A.; Lahuerta, P.; Latorre, J.; Sanau, M.; Solana, I.; Schowtzer, W. *Inorg. Chem.* **1988**, 27, 2131. (e) Fonseca, I.; Hernandez, E.; Sanz-Aparicio, J.; Terreros, P.; Torrens, H. *J. Chem. Soc., Dalton Trans.* **1994**, 781.

(23) Rodman, G. S.; Mann, K. R. *Inorg. Chem.* **1988**, 27, 3338.

(24) (a) Kiriakidou-Kazemifar, N. K.; Auca, M.; Pakkanen, T. A.; Tunik, S. P.; Nordlander, E. *J. Organomet. Chem.* **2001**, 623, 65. (b) Polo, A.; Claver, C.; Castellón, S.; Ruiz, A.; Bayón, J. C.; Real, J.; Meali, C.; Masi, D. *Organometallics* **1992**, 11, 3525. (c) Bayón, J. C.; Esteban, P.; Real, J.; Claver, C.; Polo, A.; Ruiz, A.; Castellón, S. *J. Organomet. Chem.* **1991**, 403, 393. (d) Bonet, J. J.; Thorez, A.; Maisonnat, A.; Galy, J.; Poilblanc, R. *J. Am. Chem. Soc.* **1979**, 101, 5940.

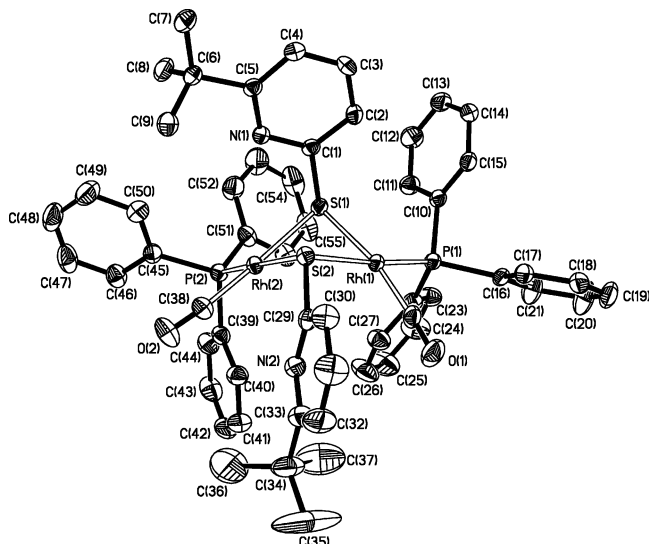


Figure 2. Molecular structure of compound $[\text{Rh}(\mu\text{-}^1\text{Bu-PyS})(\text{CO})(\text{PPh}_3)_2]$ (**5**).

compound **6** is an air-sensitive orange solid. Both complexes have been fully characterized by elemental analysis, FAB⁺ mass spectra, and NMR. In addition, the molecular structure of compound **5** has been determined by X-ray diffraction methods and is shown in Figure 2, which will be discussed in greater detail below. As in the previous four complexes **1–4**, the dinuclear structure is maintained by two 6-*tert*-butylpyridine-2-thiolate ligands with a thiolate coordination mode $\mu\text{-}(1:2\kappa^2\text{S})$; however unlike the previously discussed complexes the two thiolates adopt a relative *anti* disposition, and a *cis* disposition of the triphenylphosphine ligands is seen. The spectroscopic data obtained from solutions of the compounds **5** and **6** in C_6D_6 are in accordance with the structure found in the solid state for compound **5** with a C_s symmetry. Thus, two sharp singlets were observed for the ¹Bu groups of the two inequivalent ¹Bu-PyS[−] ligands in the ¹H NMR of both compounds. In addition, the two equivalent carbonyl ligands of compound **5** were observed as a ddd at δ 190.2 ppm ($^1J_{\text{Rh-C}} = 75.3$ Hz, $^2J_{\text{P-C}} = 17.1$ Hz, and another coupling $J = 2.9$ Hz) in the ¹³C{¹H} NMR spectrum. Further evidence for a *cis* arrangement of the two carbonyls in solution comes from the appearance of two IR bands at 1989 and 1976 cm^{-1} , whereas if the two carbonyls were *trans*, a single IR band would be seen (e.g., ref 24b).

Molecular Structures of Compounds $[\text{Ir}(\mu\text{-}^1\text{Bu-PyS})(\text{COD})_2]$ (2**) and $[\text{Rh}(\mu\text{-}^1\text{Bu-PyS})(\text{CO})(\text{PPh}_3)_2]$ (**5**).** Good-quality crystals for X-ray diffraction of compound **2** were obtained by diffusion of pentane into a concentrated solution of the complex in dichloromethane. Key bond lengths and angles are shown in Table 1, whereas collection and refinement data for all complexes in this paper are in Table 5. The structure of **2** (Figure 1) shows the *syn-endo* disposition of the two thiolates with respect to the folded Ir_2S_2 core. Coordination geometry at both Ir centers is distorted square planar, with similar acute Ir–S–Ir [76.08(6)° and 75.75(7)°] and S–Ir–S angles [74.73(7)° and 74.59(8)°], whereas the S–Ir–C angles are between 95.6(3)° and 101.4(2)°. The values for *trans*-angles S–Ir–Ct (Ct = centroid of C=C bond) are close to 180° [range 170.1(2)–174.17(7)°], but also reflect the distortion of the square-planar metal environment. The fold of the Ir_2S_2 core is 101.02(6)°,

Table 1. Selected Bond Distances (Å) and Angles (deg) for **2** and **13**

compound 2		compound 13	
Ir(1)–S(1)	2.357(2)	Rh(1)–S(1)	2.3651(9)
Ir(1)–S(2)	2.363(2)	Rh(1)–S(2)	2.3696(9)
Ir(2)–S(1)	2.358(2)	Rh(2)–S(1)	2.3617(10)
Ir(2)–S(2)	2.369(2)	Rh(2)–S(2)	2.3699(9)
Ir(1)–C(1)	2.119(8)	Rh(1)–C(1)	2.144(4)
Ir(1)–C(2)	2.093(8)	Rh(1)–C(2)	2.141(4)
Ir(1)–C(5)	2.138(9)	Rh(1)–C(5)	2.147(4)
Ir(1)–C(6)	2.112(8)	Rh(1)–C(6)	2.150(4)
Ir(2)–C(9)	2.115(8)	Rh(2)–C(9)	2.118(5)
Ir(2)–C(12)	2.120(8)	Rh(2)–C(12)	2.126(4)
Ir(2)–C(13)	2.096(8)	Rh(2)–C(13)	2.143(4)
Ir(2)–C(16)	2.121(9)	Rh(2)–C(16)	2.144(5)
S(1)–C(17)	1.795(8)	S(1)–C(17)	1.768(4)
S(2)–C(26)	1.798(9)	S(2)–C(28)	1.767(4)
S(1)–Ir(1)–S(2)	74.73(7)	S(1)–Rh(1)–S(2)	77.09(3)
S(1)–Ir(1)–Ct(1) ^a	97.6(2)	S(1)–Rh(1)–Ct(1) ^a	97.48(10)
S(1)–Ir(1)–Ct(2) ^a	171.0(2)	S(1)–Rh(1)–Ct(2) ^a	174.17(7)
S(2)–Ir(1)–Ct(1) ^a	170.8(2)	S(2)–Rh(1)–Ct(1) ^a	172.68(9)
S(2)–Ir(1)–Ct(2) ^a	101.2(2)	S(2)–Rh(1)–Ct(2) ^a	97.69(8)
Ct(1)–Ir(1)–Ct(2) ^a	87.2(3)	Ct(1)–Rh(1)–Ct(2) ^a	87.49(12)
S(1)–Ir(2)–S(2)	74.59(8)	S(1)–Rh(2)–S(2)	77.15(3)
S(1)–Ir(2)–Ct(3) ^a	101.5(2)	S(1)–Rh(2)–Ct(3) ^a	173.91(11)
S(1)–Ir(2)–Ct(4) ^a	170.6(2)	S(1)–Rh(2)–Ct(4) ^a	96.91(11)
S(2)–Ir(2)–Ct(3) ^a	170.1(2)	S(2)–Rh(2)–Ct(3) ^a	98.61(12)
S(2)–Ir(2)–Ct(4) ^a	97.7(2)	S(2)–Rh(2)–Ct(4) ^a	173.74(9)
Ct(3)–Ir(2)–Ct(4) ^a	86.9(3)	Ct(3)–Rh(2)–Ct(4) ^a	87.16(16)
Ir(1)–S(1)–Ir(2)	76.08(6)	Rh(1)–S(1)–Rh(2)	92.67(3)
Ir(1)–S(1)–C(17)	115.6(3)	Rh(1)–S(1)–C(17)	113.74(12)
Ir(2)–S(1)–C(17)	124.4(3)	Rh(2)–S(1)–C(17)	110.85(13)
Ir(1)–S(2)–Ir(2)	75.75(7)	Rh(1)–S(2)–Rh(2)	92.35(3)
Ir(1)–S(2)–C(26)	122.7(3)	Rh(1)–S(2)–C(28)	113.75(12)
Ir(2)–S(2)–C(26)	117.3(3)	Rh(2)–S(2)–C(28)	112.03(12)

^a Midpoints of the cyclooctadiene olefinic bonds: Ct(1) for C(1)=C(2), Ct(2) for C(5)=C(6), Ct(3) for C(9)=C(16), and Ct(4) for C(12)=C(13).

Table 2. Selected Bond Distances (Å) and Angles (deg) for **5**

Rh(1)–S(1)	2.3910(6)	Rh(2)–S(1)	2.3914(6)
Rh(1)–S(2)	2.3809(6)	Rh(2)–S(2)	2.3646(6)
Rh(1)–P(1)	2.2598(6)	Rh(2)–P(2)	2.2514(6)
Rh(1)–C(28)	1.825(2)	Rh(2)–C(38)	1.837(2)
S(1)–C(1)	1.793(2)	S(2)–C(29)	1.793(2)
C(28)–O(1)	1.152(3)	C(38)–O(2)	1.140(3)
S(1)–Rh(1)–S(2)	81.81(2)	S(1)–Rh(2)–S(2)	82.136(19)
S(1)–Rh(1)–P(1)	90.63(2)	S(1)–Rh(2)–P(2)	92.71(2)
S(1)–Rh(1)–C(28)	169.60(8)	S(1)–Rh(2)–C(38)	175.81(8)
S(2)–Rh(1)–P(1)	172.42(2)	S(2)–Rh(2)–P(2)	173.60(2)
S(2)–Rh(1)–C(28)	93.82(7)	S(2)–Rh(2)–C(38)	95.16(7)
P(1)–Rh(1)–C(28)	93.73(7)	P(2)–Rh(2)–C(38)	90.20(7)
Rh(1)–S(1)–Rh(2)	80.779(19)	Rh(2)–S(2)–Rh(1)	81.538(18)
Rh(1)–S(1)–C(1)	106.39(7)	Rh(2)–S(2)–C(29)	112.42(8)
Rh(2)–S(1)–C(1)	103.68(7)	Rh(1)–S(2)–C(29)	105.91(7)
Rh(1)–C(28)–O(1)	176.6(2)	Rh(2)–C(38)–O(2)	175.0(2)

and the Ir–Ir separation 2.9055(8) Å. Among related Ir complexes, this metal–metal separation is rather small. The closest analogue to **2** characterized by X-ray diffraction is $[\text{Ir}(\mu\text{-PhS})(\text{COD})_2]_2$,^{22d} in which the Ir–Ir distance is 3.181(1) Å. The two complexes are similar in their Ir–S bond distances: for **2** the range is 2.357–2.369(2) Å, average 2.362(1) Å, whereas in $[\text{Ir}(\mu\text{-PhS})(\text{COD})_2]_2$,^{22d} the average value is 2.345(7) Å. In the related complex $[\text{Ir}(\mu\text{-SCH}_2\text{CH}_2\text{CH}_2\text{NMe}_2)(\text{COD})_2]_2$,^{22b} Ir–S distances were very similar [average 2.340(2) Å], whereas the metal–metal distance [2.946(1) Å] was not quite as short as that in **2**. Finally, in $[\text{Ir}(\mu\text{-SC}_6\text{F}_5)(\text{COD})_2]_2$,^{22e} even though thiolates are very electron-withdrawing, the Ir–S distances [range 2.375(2)–2.402(3) Å, average 2.390(2) Å] and Ir–Ir distance (3.066(1) Å) are more similar to those in the SPn analogue.

Suitable crystals for X-ray diffraction of compound **5** were grown by diffusion of methanol into a concentrated solution of

Table 3. Selected Bond Distances (Å) and Angles (deg) for 7^a

Rh(1)–S(1)	2.4024(12)	2.3969(11)	Rh(2)–S(1)	2.3535(12)	2.3500(12)
Rh(1)–S(2)	2.3715(12)	2.3727(12)	Rh(2)–N(3)	2.125(5)	2.138(4)
Rh(1)–C(1)	2.136(5)	2.143(5)	Rh(2)–C(9)	2.147(6)	2.148(5)
Rh(1)–C(2)	2.156(5)	2.126(5)	Rh(2)–C(10)	2.126(5)	2.105(5)
Rh(1)–C(5)	2.125(5)	2.135(5)	Rh(2)–C(13)	2.168(8) ^b	2.125(5)
Rh(1)–C(6)	2.137(5)	2.126(5)	Rh(2)–C(14)	2.182(8) ^b	2.137(5)
S(1)–C(17)	1.763(4)	1.752(4)	S(2)–C(25)	1.729(5)	1.726(5)
N(1)–C(17)	1.309(5)	1.318(6)	N(3)–C(25)	1.325(6)	1.331(6)
N(2)–C(17)	1.366(5)	1.364(6)	N(4)–C(25)	1.352(6)	1.354(6)
C(1)–C(2)	1.386(8)	1.384(8)	C(9)–C(10)	1.378(9)	1.400(8)
C(5)–C(6)	1.371(8)	1.392(9)	C(13)–C(14)	1.404(12) ^b	1.389(9)
S(1)–Rh(1)–S(2)	96.19(4)	95.71(4)	S(1)–Rh(2)–N(3)	81.48(13)	80.85(12)
S(1)–Rh(1)–Ct(1) ^c	94.30(11)	94.69(11)	S(1)–Rh(2)–Ct(3) ^c	100.44(13)	100.55(10)
S(1)–Rh(1)–Ct(2) ^c	178.24(12)	177.77(13)	S(1)–Rh(2)–Ct(4) ^{b,c}	165.8(2)	165.97(14)
S(2)–Rh(1)–Ct(1) ^c	168.70(12)	169.53(12)	N(3)–Rh(2)–Ct(3) ^c	173.18(17)	165.41(16)
S(2)–Rh(1)–Ct(2) ^c	83.42(12)	82.95(14)	N(3)–Rh(2)–Ct(4) ^{b,c}	93.4(3)	93.97(18)
Ct(1)–Rh(1)–Ct(2) ^c	86.21(16)	86.61(17)	Ct(3)–Rh(2)–Ct(4) ^{b,c}	86.2(3)	87.76(17)
Rh(1)–S(1)–Rh(2)	88.50(4)	87.60(4)	Rh(1)–S(2)–C(25)	112.39(17)	111.71(17)
Rh(1)–S(1)–C(17)	110.92(16)	111.69(17)	Rh(2)–N(3)–C(25)	115.5(4)	115.7(3)
Rh(2)–S(1)–C(17)	117.06(16)	116.33(17)	Rh(2)–N(3)–C(26)	138.5(4)	137.4(4)
S(1)–C(17)–N(1)	128.1(4)	127.4(4)	S(2)–C(25)–N(3)	126.6(4)	126.1(4)
S(1)–C(17)–N(2)	120.3(4)	121.5(4)	S(2)–C(25)–N(4)	123.3(4)	123.7(4)
N(1)–C(17)–N(2)	111.6(4)	111.1(4)	N(3)–C(25)–N(4)	110.1(4)	110.1(4)

^a Two crystallographically independent molecules were observed in the crystal. ^b Olefinic atoms C(13) and C(14) exhibited static disorder; mean values for the two disordered moieties are stated in the table. ^c Midpoints of the cyclooctadiene olefinic bonds: Ct(1), C(1)=C(2); Ct(2), C(5)=C(6); Ct(3), C(9)=C(10); and Ct(4), C(13)=C(14).

Table 4. Selected Bond Distances (Å) and Angles (deg) for 18

Ir–P	2.2342(12)	Ir–S	2.4095(13)
Ir–N(1)	2.125(3)	Ir–C(1)	1.816(5)
S–C(2)	1.749(4)	N(1)–C(2)	1.324(5)
C(1)–O(1)	1.163(5)	N(2)–C(2)	1.350(5)
P–Ir–S	97.67(4)	Ir–N(1)–C(2)	99.0(2)
P–Ir–N(1)	166.37(9)	Ir–N(1)–C(4)	152.4(3)
P–Ir–C(1)	90.08(14)	C(2)–N(1)–C(4)	107.5(3)
S–Ir–N(1)	68.83(9)	Ir–C(1)–O	176.2(5)
S–Ir–C(1)	169.70(14)	S–C(2)–N(1)	113.0(3)
N(1)–Ir(1)–C(1)	103.54(16)	S–C(2)–N(2)	135.3(3)
Ir–S–C(2)	78.22(13)	N(1)–C(2)–N(2)	111.7(3)

the complex in dichloromethane. Key bond lengths and angles are shown in Table 2. Like **2**, **5** (Figure 2) shows a folded Rh₂S₂ core, with both Rh atoms in distorted square-planar coordination geometry, and the thiolate *cis* to both small CO ligands [bonded through S(2)] is *endo* to the Rh₂S₂ core. The sums of the four bond angles between pairs of *cis* ligands around each metal add up to 360.0°, within experimental uncertainty. In contrast to **2**, **5** shows an *anti* disposition of the two thiolates, with the thiolate flanked by the large PPh₃ ligands occupying the *exo* position with respect to the Rh₂S₂ core. The greatest distortions from square-planar geometry consist of the small S–Rh–S angles [81.81(2)° and 82.136(19)°]. In addition, the S–Rh–CO angles involving S(2) are the largest [95.16(7)° and 93.82(7)°], followed by the other intraligand *cis* angles. As for Rh–S bond distances, those *trans* to the CO ligands [Rh(1)–S(1) 2.3910(6) Å and Rh(2)–S(1) 2.3914(6) Å] are slightly longer than those *trans* to the phosphines [Rh(1)–S(2) 2.3809(6) Å and Rh(2)–S(2) 2.3646(6) Å], a phenomenon seen in the analogous complex with PhS[−] ligands.^{25d} The shape of the complex, including the relative *cis* disposition of the phosphines and the *anti* disposition of thiolates, as well as its metrical parameters, are very similar to those of literature complexes that have been structurally characterized.^{25a–d}

Complexes Derived from 1-Methyl-4-tert-butylimidazole-2-thiol (Me-^tBu-ImSH) and Molecular Structure of 7. The complexes [Rh(μ -Me-^tBu-ImS)(COD)]₂ (**7**, Scheme 3) and [Ir-

(μ -Me-^tBu-ImS)(COD)]₂ (**8**) were obtained from the reaction of the dinuclear compounds [M(μ -OMe)(COD)]₂ with 1-methyl-4-tert-butylimidazole-2-thiol (Me-^tBu-ImSH) in dichloromethane. The compounds were isolated as orange and red microcrystalline solids in good yield and have been characterized by elemental analysis, FAB⁺ spectra, and spectroscopic methods. The FAB⁺ spectra of both compounds showed the dinuclear ions at *m/z* 760 and 939, respectively. The ¹H NMR spectrum in CDCl₃ or CD₂Cl₂ at RT for compound **7** showed broadened resonances for every type of proton, which suggested fluxional behavior. Thus, the =CH and >CH₂ protons of the COD ligands were observed in CD₂Cl₂ as a resonance at δ 4.59 ppm and two resonances at δ 2.47 and 1.93 ppm, respectively. Moreover, three resonances at δ 6.50, 3.45, and 1.28 ppm were observed for the Me-^tBu-ImS[−] ligands, which correspond to the =CH, N-CH₃, and ^tBu protons, respectively.

To establish the coordination mode of the bridging 1-methyl-4-tert-butylimidazole-2-thiolate ligands in the dinuclear compounds, variable-temperature ¹H analysis was carried out on both complexes. The ¹H NMR spectrum of compound [Ir(μ -Me-^tBu-ImS)(COD)]₂ (**8**) in toluene-*d*₈ at RT consisted of featureless resonances except for the =CH resonance of the Me-^tBu-ImS[−] ligands, which was observed as a sharp singlet at δ 5.99 ppm. On warming, well-defined resonances resulted, and at 70 °C the spectrum closely resembled that of compound **7** at RT (Figure 3a). More conclusive results came from the ¹H NMR spectrum of **8** at −60 °C that evidence the lack of symmetry in the molecule (Figure 3b). Thus, six distinct singlets were observed at δ 5.75 and 5.62 ppm, 2.92 and 2.54 ppm, and 1.64 and 1.32 ppm for the =CH, N-Me, and ^tBu protons, respectively, of the inequivalent Me-^tBu-ImS[−] ligands. In addition, eight different resonances were observed for the =CH protons of the inequivalent COD ligands that could be grouped in four sets, corresponding to the four HC=CH olefin fragments, with the

(25) References to structures of complexes like **5**: (a) Dilworth, J. R.; Morales, D.; Zheng, Y. *J. Chem. Soc., Dalton Trans.* **2000**, 3017. (b) Schumann, H.; Hemling, N.; Goren, N.; Blue, J. *J. Organomet. Chem.* **1995**, 485, 209. (c) Jones, R. A.; Schwab, S. T. *J. Crystallogr. Spectrosc.* **1986**, 16, 577. (d) Bonet, J. J.; Kalck, P.; Poilblanc, R. *Inorg. Chem.* **1977**, 16, 1514. (e) Osakada, K.; Matsumoto, K.; Yamamoto, T.; Yamamoto, A. *Organometallics* **1985**, 4, 857.

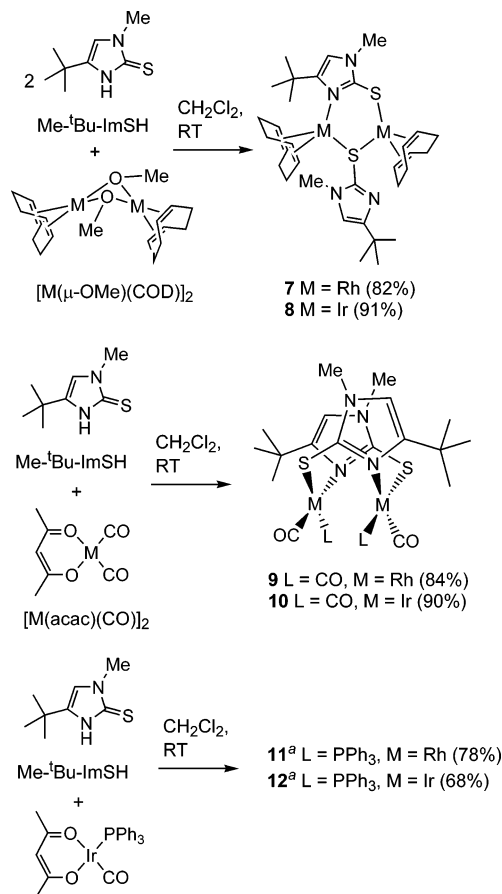
Table 5. Data Collection and Refinement for Structures of 2, 5, 7, 13, and 18

	2	5	7	13	18
mol. formula	C ₃₄ H ₄₈ Ir ₂ N ₂ S ₂	C ₅₆ H ₅₄ N ₂ O ₂ P ₂ Rh ₂ S ₂	C ₃₂ H ₅₀ N ₄ Rh ₂ S ₂	C ₃₉ H ₆₆ N ₄ ORh ₂ S ₂	C ₃₀ H ₃₄ IrN ₂ OPS
MW	933.26	1118.89	760.7	876.90	693.82
cryst dimens (mm)	0.29×0.05×0.05	0.31×0.17×0.10	0.21×0.12×0.05	0.12×0.11×0.03	0.16×0.13×0.05
cryst syst	monoclinic	triclinic	triclinic	monoclinic	triclinic
space group	<i>P</i> 2 ₁ / <i>c</i>	<i>P</i> $\bar{1}$	<i>P</i> $\bar{1}$	<i>P</i> 2 ₁ / <i>n</i>	<i>P</i> $\bar{1}$
<i>a</i> (Å)	11.665(3)	12.0428(14)	11.2689(9)	10.4217(7)	9.243(5)
<i>b</i> (Å)	28.630(7)	12.7050(14)	16.9773(14)	20.8686(14)	9.618(5)
<i>c</i> (Å)	11.170(3)	18.720(2)	18.2119(15)	18.8799(12)	16.901(5)
α (deg)	90.00	81.561(2)	101.9520(10)	90.00	99.912(5)
β (deg)	117.252(5)	72.552(2)	105.6020(10)	96.6200(10)	94.141(5)
γ (deg)	90.00	69.439(2)	90.2450(10)	90.00	104.632(5)
<i>V</i> (Å ³)	3316.4(14)	2555.7(5)	3276.4(5)	4078.7(5)	1421.5(11)
<i>Z</i>	4	2	4	4	2
<i>D</i> _{calc} (g cm ⁻³)	1.869	1.454	1.542	1.428	1.621
μ (mm ⁻¹)	8.168	0.833	1.162	0.946	4.851
min. max. transmn factor	0.312, 0.667	0.779, 0.921	0.790, 0.941	0.896, 0.975	0.495, 0.784
2 θ _{max} (deg)	57.52	57.68	57.52	57.70	57.42
no. of measd rflns	22228	31989	40642	27234	17587
no. of indep rflns	7937 [<i>R</i> (int) = 0.0652]	12 188 [<i>R</i> (int) = 0.0309]	15 513 [<i>R</i> (int) = 0.0271]	9767 [<i>R</i> (int) = 0.0346]	6712 [<i>R</i> (int) = 0.0368]
no. of intense rflns with <i>I</i> > 2 σ (<i>I</i>)	5605	10417	12855	8056	5954
no. of params	378	776	724	615	429
<i>R</i> (<i>F</i>) intense, all (%)	5.32, 8.72	3.15, 3.97	5.20, 6.52	4.44, 5.77	3.18, 3.92
w <i>R</i> (<i>F</i> ²) intense, all (%)	8.90, 9.89	7.12, 7.45	11.92, 12.58	10.33, 11.03	6.27, 6.50
GOF	1.025	1.024	1.063	1.037	1.046

help of the ¹H–¹H COSY spectrum. In experiments of this kind, generally toluene-*d*₈ led to greater chemical shift differences for the =CH protons of coordinated COD ligands than did CD₂-Cl₂, but there was no obvious solvent dependence on equilibria at the same temperature.

Compound **7** undergoes a similar dynamic behavior, although the coalescence temperature was lower than that found for complex **8**, as might be expected for a second-row congener. Interestingly, the ¹H NMR spectrum of compound **7** in CD₂Cl₂ at –95 °C was similar to that of **8** at –60 °C: for the two inequivalent Me-^tBu-ImS[–] ligands, a total of six singlets were seen, and for the =CH protons of the COD ligands, seven broad resonances (two overlapping) were identified with the help of the ¹H–¹H COSY spectrum.

Suitable crystals for X-ray diffraction of compound **7** were obtained by cooling a concentrated solution of the complex in *n*-hexane. The ORTEP diagram of one of the two crystallographically independent—but chemically analogous—molecules is shown in Figure 4, and key bond lengths and angles are collected in Table 3. Although **7** is dinuclear with the two metal centers bridged by two thiolate ligands, one ligand is in μ -(1 κ S,2 κ N) coordination mode, which makes the complex unsymmetrical (cf. **C**, Chart 1). Both Rh centers feature distorted square-planar geometry. Looking at the bonding of the six-membered Rh–S–Rh–SCN ring at the core of the complex, the angle Rh(1)–S(1)–Rh(2) of the thiolate in μ -(1:2 κ^2 S) coordination mode is 88.05(4)°, about 12° more open than the corresponding angles in **2** (Table 1), presumably a consequence of the presence of the second thiolate in μ -(1 κ S,2 κ N) coordination and the larger size of the central ring. The intraligand *cis* angles at each Rh center, S(1)–Rh(1)–S(2) [mean 95.95(3)°] and S(1)–Rh(2)–N(3) [mean 81.17(9)°], are also significantly larger than the corresponding 74.59(8)° and 74.73(7)° angles in the Ir₂S₂ core of **2**. Looking at bond distances, the Rh(1)–S(1) distance [2.3997(8) Å] is approximately 0.05 Å longer than the Rh(2)–S(1) one [2.3518(9) Å], and Rh(1)–S(2) is between both of these [2.3721(9) Å]. A survey of the literature highlights complex [Rh(μ -PyS)(tfbb)]₂,^{13b} for which a crystal structure revealed μ -(1 κ S,2 κ N) and μ -(1:2 κ^2 S) coordination, with

Scheme 3. Syntheses of Me-^tBu-ImS Complexes

^a Stoichiometry is certain; structure is tentative. See text.

similar key angles in the six-membered core ring and similar bond distances. To our knowledge, there is no other structurally characterized dinuclear complex of pyridine- or imidazole-thiolates or their benzo or saturated derivatives with such a structure, so further comparisons are impossible.

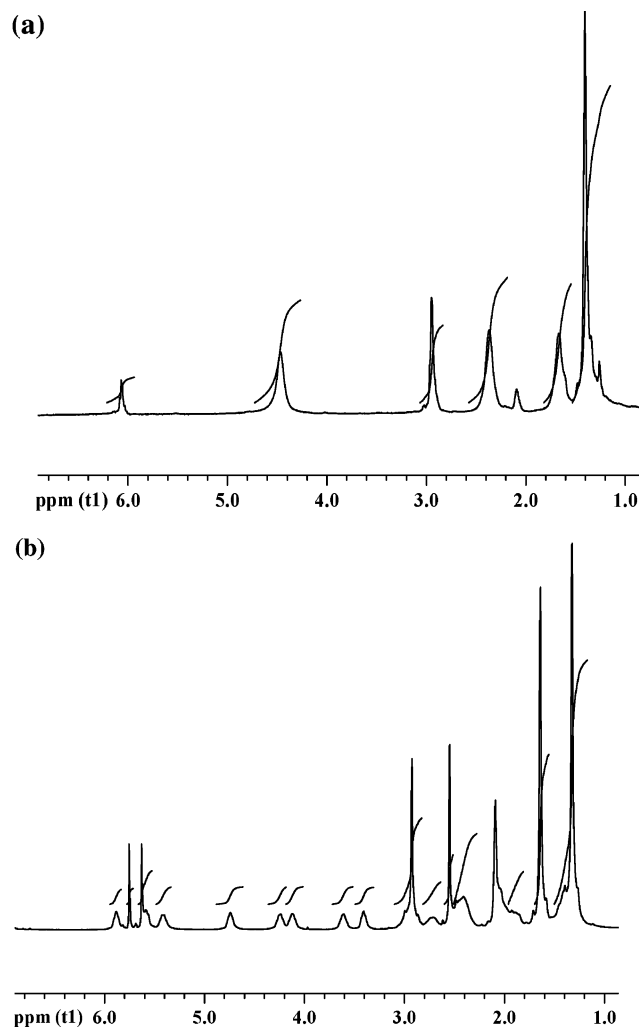


Figure 3. ^1H NMR spectra of compound $[\text{Ir}(\mu\text{-Me-}^1\text{Bu-ImS})(\text{cod})]_2$ (**8**) in toluene- d_8 at (a) 70 °C and (b) -60 °C.

The NMR spectroscopic data for both **7** and **8** at low temperature are compatible with the unsymmetrical dinuclear structure revealed by solid-state data in Figure 4. On the other hand, the data at higher temperatures can be explained by switching of the coordination modes of the bridging ligands. Possible pathways in this dynamic equilibrium (Scheme 4) could include symmetrical dinuclear species having bis- μ -(1:2 $\kappa^2\text{S}$) or bis- μ -(1 $\kappa\text{S},2\kappa\text{N}$) (either a *cis* head-to-tail or head-to-head isomer) coordinated bridging ligands.^{13b}

The direct protonation of the acetylacetonate ligands in the mononuclear complexes $[\text{M}(\text{acac})(\text{CO})_2]$ ($\text{M} = \text{Rh}, \text{Ir}$) with 1-methyl-4-*tert*-butylimidazole-2-thiol ($\text{Me-}^1\text{Bu-ImSH}$) resulted in the formation of the dinuclear complexes $[\text{Rh}(\mu\text{-Me-}^1\text{Bu-ImS})(\text{CO})_2]_2$ (**9**, Scheme 3) and $[\text{Ir}(\mu\text{-Me-}^1\text{Bu-ImS})(\text{CO})_2]_2$ (**10**), which were isolated as orange and dark purple microcrystalline solids in high yield. The dinuclear formulation of the compounds is sustained by the IR and the FAB+ spectra, which showed several dinuclear ions. In particular, the IR spectra of both compounds in dichloromethane showed three $\nu(\text{CO})$ bands for the terminal carbonyl groups at 2077 (s), 2057 (m), and 2005 (s) cm^{-1} (**9**) and 2068 (s), 2041 (m), and 1990 (s) cm^{-1} (**10**). This pattern and their relative intensities (s, m, s) are characteristic of dinuclear complexes with an approximately face-to-face disposition of both metal coordination planes resulting from a μ -(1 $\kappa\text{S},2\kappa\text{N}$) coordination mode of both $\text{Me-}^1\text{Bu-ImS}^-$ bridging ligands located in a relative *cis* position.²⁶

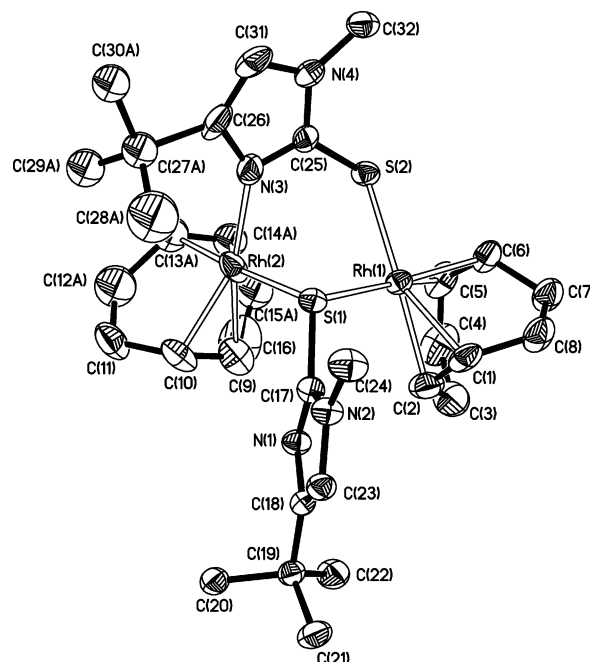
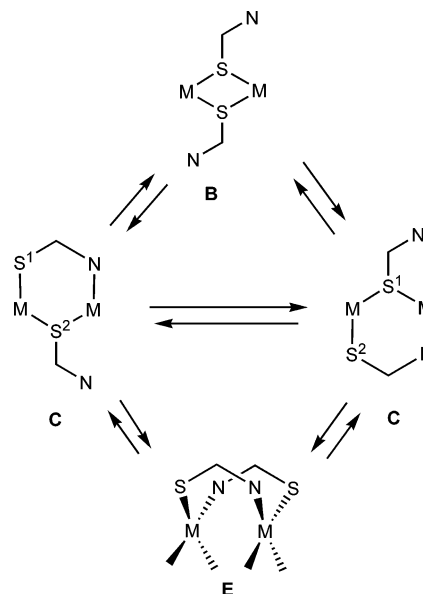


Figure 4. Molecular structure of compound $[\text{Rh}(\mu\text{-Me-}^1\text{Bu-ImS})(\text{COD})]_2$ (**7**).

Scheme 4. Possible Pathways Responsible for the Fluxional Behavior of Complexes $[\text{M}(\mu\text{-Me-}^1\text{Bu-ImS})(\text{COD})]_2$ ($\text{M} = \text{Rh}$, **7; Ir , **8**): bis- μ -(1:2 $\kappa^2\text{S}$) (**B**) \rightleftharpoons μ -(1 $\kappa\text{S},2\kappa\text{N}$)- μ -(1:2 $\kappa^2\text{S}$) (**C**) \rightleftharpoons HT-bis- μ -(1 $\kappa\text{S},2\kappa\text{N}$) (**E**)**



The compound $[\text{Ir}(\mu\text{-Me-}^1\text{Bu-ImS})(\text{CO})_2]_2$ (**10**) is apparently rigid since no changes were observed in the ^1H and $^{13}\text{C}\{^1\text{H}\}$ NMR spectra between -50 and 25 °C. The spectroscopic information evidenced equivalent $\text{Me-}^1\text{Bu-ImS}^-$ bridging ligands, and interestingly, two distinct resonances for the carbonyl ligands were observed in the $^{13}\text{C}\{^1\text{H}\}$ NMR spectrum at δ 173.5 and 172.2 ppm. These data would be consistent with either a head-to-head (*cis*-HH) or head-to-tail (*cis*-HT) structure with C_s and C_2 symmetry, respectively. In sharp contrast, the compound $[\text{Rh}(\mu\text{-Me-}^1\text{Bu-ImS})(\text{CO})_2]_2$ (**9**) is dynamic, as can

(26) (a) Connelly, N. G.; Finn, C. J.; Freeman, M. K.; Orpen, G. A.; Stirling, J. *J. Chem. Soc., Chem. Commun.* **1984**, 1025. (b) Mannotti-Lanfredi, A.; Tiripicchio, A.; Uson, R.; Oro, L. A.; Ciriano, M. A.; Villarroya, B. E. *Inorg. Chim. Acta* **1984**, 88, L9.

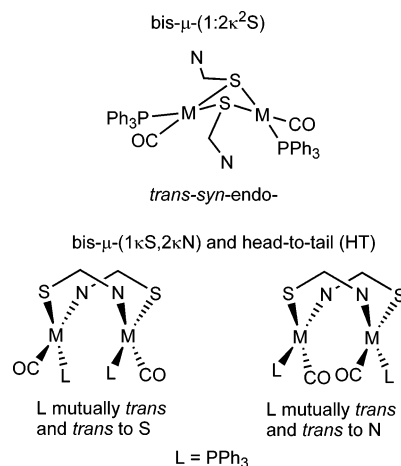
be observed in the $^{13}\text{C}\{^1\text{H}\}$ NMR spectrum, but not in the ^1H NMR spectrum, which remains unchanged in the range of temperatures under study and shows equivalent bridging ligands. It is noticeable that the carbonyl ligands were not observed in the $^{13}\text{C}\{^1\text{H}\}$ NMR spectrum in chloroform at room temperature. However, on cooling to $-50\text{ }^\circ\text{C}$, two doublets at δ 186.7 (d, $J_{\text{C-Rh}} = 64.8\text{ Hz}$) and 182.8 (d, $J_{\text{C-Rh}} = 68.7\text{ Hz}$), corresponding to two sets of equivalent carbonyl ligands, were observed. On warming, a broad doublet resonance at δ 185.10 (d, $J_{\text{Rh-C}} = 68.7\text{ Hz}$) was observed in toluene- d_8 at $80\text{ }^\circ\text{C}$ as a consequence of the scrambling of the carbonyl ligands that became equivalent at high temperature. This dynamic behavior is not involving the fragmentation of the dinuclear framework, as the molecular weight determined in chloroform at RT is in agreement with that expected for a dinuclear formulation. Thus, the more reasonable explanation for the observed scrambling is the interconversion, from $\mu\text{-}(1\kappa\text{S},2\kappa\text{N})$ to $\mu\text{-}(1:2\kappa^2\text{S})$, of the coordination mode of both Me- $^t\text{Bu-ImS}^-$ bridging ligands.^{13b}

It is noteworthy that compounds **9** and **10** exist as a single isomer. The spectroscopic data of both compounds at low temperature are identical and should have the same *cis*-HH or *cis*-HT structure. However, the *cis*-HT structure is preferred over the *cis*-HH because of the steric repulsion between the ^tBu groups in the latter structure.

The reaction of $[\text{M}(\text{acac})(\text{CO})(\text{PPh}_3)]$ ($\text{M} = \text{Rh}, \text{Ir}$) with 1-methyl-4-*tert*-butylimidazole-2-thiol (Me- $^t\text{Bu-ImSH}$) in dichloromethane gave orange solutions of the complexes $[\text{Rh}(\mu\text{-Me-}^t\text{Bu-ImS})(\text{CO})(\text{PPh}_3)]_2$ (**11**, Scheme 3) and $[\text{Ir}(\mu\text{-Me-}^t\text{Bu-ImS})(\text{CO})(\text{PPh}_3)]_2$ (**12**), which were isolated as orange solids, after recrystallization from dichloromethane/methanol, in moderate yield. Both complexes are air-sensitive solids that slowly decompose in solution, which precluded a reliable determination of the molecular weight in solution. Nevertheless, the FAB+ spectra of both complexes showed the molecular ions as well as other dinuclear ions that resulted from the sequential loss of carbonyl and triphenylphosphine ligands. The IR spectra of both compounds consisted of a strong $\nu(\text{CO})$ band for the terminal carbonyl groups at 1974 and 1973 cm^{-1} , respectively.

Compound **12** exists at $-60\text{ }^\circ\text{C}$ as a single isomer with equivalent triphenylphosphine ligands, as evidenced by the $^{31}\text{P}\{^1\text{H}\}$ NMR spectrum in toluene- d_8 , which showed a single resonance at δ 22.13 ppm. The ^1H NMR at the same temperature showed three resonances at δ 5.33, 2.54, and 1.43 for the equivalent Me- $^t\text{Bu-ImS}^-$ ligands. On warming, a second negligible isomer is observed in the $^{31}\text{P}\{^1\text{H}\}$ NMR spectrum at δ 17.95 ppm. However, the main difference was observed in the aromatic region of the spectrum: at room temperature, two averaged resonances for the triphenylphosphine protons were seen, which at $-60\text{ }^\circ\text{C}$ resolved into a set of nine well-defined multiplets that spread out between 9 and 7.1 ppm. On the other hand, no significant change in the chemical shift of the phosphorus resonance was observed at low temperature. The $^{31}\text{P}\{^1\text{H}\}$ NMR spectrum of compound **11** in toluene- d_8 at RT showed the presence of a main isomer at δ 38.7 ppm ($J_{\text{Rh-P}} = 161.4\text{ Hz}$) together with a minor isomer (ca. 10%) at δ 40.6 ppm ($J_{\text{Rh-P}} = 165.0\text{ Hz}$). Although the ratio between the two isomers is approximately the same at $-60\text{ }^\circ\text{C}$ ($\approx 10:1$), the signal for the minor isomer is shifted to higher frequency and was found at δ 49.9 ppm with a similar coupling constant ($J_{\text{Rh-P}} = 163.7\text{ Hz}$). Interestingly, the same temperature effect on the triphenylphosphine protons described above for the iridium compound was observed at $-60\text{ }^\circ\text{C}$ for compound **11**, pointing to similar structures and fluxionality for **11** and **12**.

Scheme 5. Possible Structures for **11** and **12**



The spectroscopic data for both compounds showing the equivalence of the bridging thiolates are compatible with both a *syn*-bis- $\mu\text{-}(1:2\kappa^2\text{S})$ and a bis- $\mu\text{-}(1\kappa\text{S},2\kappa\text{N})$ (*cis*-HT) structure (Scheme 5). As far as the relative disposition of the bulky triphenylphosphine ligands is concerned, only the *trans* (C_2) arrangement is possible in the bis-thiolate structure, whereas in the head-to-tail case, either of two *trans* isomers (C_2 symmetry) are possible. Despite the dynamic behavior, which could be associated with the restricted rotation of the phenyl rings in the PPh_3 ligands at low temperature, both complexes seem to have rigid structures since no changes in the coordination mode of the bridging ligands have been observed (^{31}P NMR evidence).

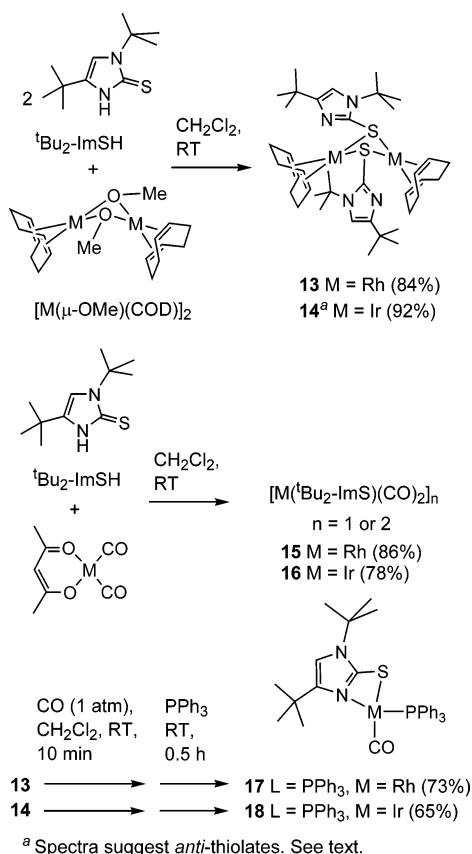
Dinuclear compounds containing benzothiazole-2-thiolate (bzta^-) or 2-mercaptobenzothiazolate (tzdt^-) ligands such as $[\text{Rh}(\mu\text{-bzta})(\text{CO})(\text{PPh}_3)]_2$ ²⁷ or $[\text{Rh}(\mu\text{-tzdt})(\text{CO})(\text{PR}_3)]_2$ ($\text{R} = \text{Me}, \text{Ph}$)^{28a} show rigid structures derived from a *cis*-HT arrangement of the bridging ligands with a *trans* disposition of the PR_3 ligands, which are located *trans* to the sulfur donor atoms. It is noticeable that the *cis* isomer was not observed in solution, in contrast with the chemistry of related dinuclear thiolate-bridged species $[\text{Rh}(\mu\text{-SR})(\text{CO})(\text{PR}_3)]_2$ where both isomers are usually observed in solution.^{25d,e} However, it is worth mentioning that the compound $[\text{Rh}(\mu\text{-SPy})(\text{CO})(\text{PPh}_3)]_2$, with an analogous structure in the solid state, is dynamic in solution and several species coexist in equilibrium that are solvent and temperature dependent.^{13c} Having in mind the above considerations we believe that complexes **11** and **12** have a *cis*-HT structures with C_2 symmetry. In addition, the observed coupling constant $J_{\text{Rh-P}}$ for complex **11** is in good agreement with *trans* $\text{Ph}_3\text{P-Rh-S}$ bonds ($J_{\text{Rh-P}} \approx 160\text{--}162\text{ Hz}$).²⁸

Complexes Derived from 1,4-Di-*tert*-butylimidazole-2-thiol ($^t\text{Bu}_2\text{-ImSH}$). The deprotonation of 1,4-di-*tert*-butylimidazole-2-thiol ($^t\text{Bu}_2\text{-ImSH}$) by the methoxo bridges of the complexes $[\text{M}(\mu\text{-OMe})(\text{COD})]_2$ ($\text{M} = \text{Rh}, \text{Ir}$) resulted in the formation of the complexes $[\text{Rh}(\mu\text{-}^t\text{Bu}_2\text{-ImS})(\text{COD})]_n$ (**13**, Scheme 6) and $[\text{Ir}(\mu\text{-}^t\text{Bu}_2\text{-ImS})(\text{COD})]_2$ (**14**), which were isolated as yellow and red microcrystalline solids in good yield.

The molecular structure of compound $[\text{Rh}(\mu\text{-}^t\text{Bu}_2\text{-ImS})(\text{COD})]_2$ (**13**) has been determined by X-ray diffraction methods and is shown in Figure 5, which will be discussed further below. Compound **13** is dinuclear in the solid state and exhibits a thiolate $\mu\text{-}(1:2\kappa^2\text{S})$ coordination mode of both $^t\text{Bu}_2\text{-ImS}^-$ ligands

(27) Ciriano, M. A.; Pérez-Torrente, J. J.; Lahoz, F. J.; Oro, L. A. *J. Organomet. Chem.* **1993**, 455, 225.

(28) (a) Cowie, M.; Sielisch, T. *J. Organomet. Chem.* **1988**, 348, 241.
(b) Ciriano, M. A.; Pérez-Torrente, J. J.; Casado, M. A.; Lahoz, F. J.; Oro, L. A. *Inorg. Chem.* **1996**, 35, 1782.

Scheme 6. Syntheses of $\mu\text{-Bu}_2\text{-ImS}$ Complexes

with a *syn-endo* disposition. The ^1H NMR spectrum in toluene- d_8 at -60°C is in agreement with the structure found in the solid state, since a single resonance for the H^5 protons of the equivalent $\mu\text{-Bu}_2\text{-ImS}^-$ bridging ligands and two resonances of the same intensity for the $=\text{CH}$ protons of the COD ligands were observed. However, the compound is fluxional, as evidenced by the ^1H NMR in CD_2Cl_2 at RT, which showed mainly featureless resonances probably due to a dynamic process involving the inversion of the Rh_2S_2 ring. Interestingly, a new static species was observed showing sharp resonances at δ 6.21, 1.56, and 1.08 for the $\mu\text{-Bu}_2\text{-ImS}^-$ protons. Taking into account that the molecular weight measured in chloroform is lower than that expected for a dinuclear formulation (508 vs 844), we suggest that the dinuclear species is in equilibrium with approximately 15% of the mononuclear compound $[\text{Rh}(\mu\text{-Bu}_2\text{-ImS})(\text{COD})]$ (Scheme 7) at RT, as deduced from the relative integrals in the ^1H NMR spectrum. This proposal is supported by the FAB+ mass spectrum, which, in addition to the dinuclear ion $[\text{Rh}(\mu\text{-Bu}_2\text{-ImS})(\text{COD})]_2^+$ at m/z 844 (11%), also shows the mononuclear ion $[\text{Rh}(\mu\text{-Bu}_2\text{-ImS})(\text{COD})]^+$ at m/z 422 (100%). Further support comes from the $^{13}\text{C}\{^1\text{H}\}$ NMR spectrum in CD_2Cl_2 at RT, where the resonances of $[\text{Rh}(\mu\text{-Bu}_2\text{-ImS})(\text{COD})]$ are observed at chemical shifts comparable to that found for related mononuclear complexes (see below).

The ^1H NMR spectra of compound $[\text{Ir}(\mu\text{-Bu}_2\text{-ImS})(\text{COD})]_2$ (**14**) in CD_2Cl_2 at -95°C or in toluene- d_8 at -80°C are comparable to that observed for compound **8** and are in accordance with a dinuclear structure having two bridging ligands with $\mu\text{-}(1\kappa\text{S},2\kappa\text{N})$ and $\mu\text{-}(1:2\kappa^2\text{S})$ coordination modes, respectively. However, the ^1H NMR spectrum at RT is not compatible with the expected dynamic behavior of this type of complexes. On the contrary, two broad singlets for the H^5 protons of the $\mu\text{-Bu}_2\text{-ImS}^-$ ligands and two broad resonances for the $=\text{CH}$ protons of the COD ligands were observed in $\text{CD}_2\text{-}$

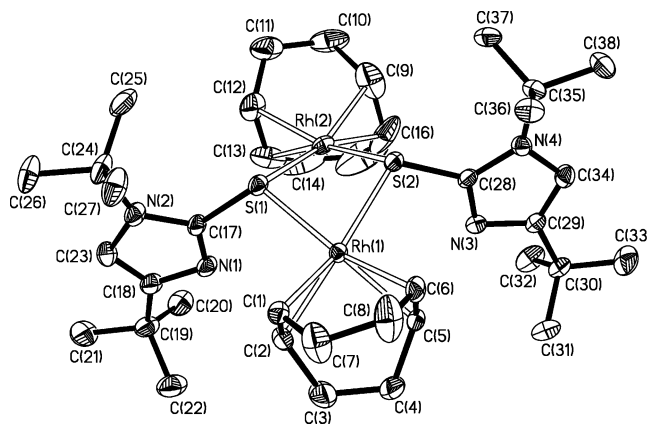
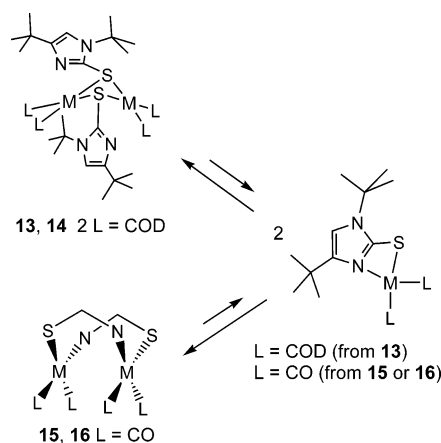


Figure 5. Molecular structure of compound $[\text{Rh}(\mu\text{-Bu}_2\text{-ImS})(\text{COD})]_2$ (**13**).

Scheme 7. Proposed Dimer–Monomer Equilibrium Involving **13–16**

Cl_2 . The inequivalence of the bridging ligands suggests a dinuclear structure having two thiolate-coordinated ($1:2\kappa^2\text{S}$)- $\mu\text{-Bu}_2\text{-ImS}^-$ ligands with an *anti* disposition. Moreover, the inversion of the Ir_2S_2 ring (ring-flipping) easily explains the number of resonances observed for the olefinic protons of the COD ligands.²⁹ It is worth mentioning that the ^1H NMR spectrum also shows minor resonances at δ 6.67 and 6.05 ppm, which correspond to other unidentified isomers (<10%).

The reaction of $[\text{M}(\text{acac})(\text{CO})_2]$ (M = Rh, Ir) with 1,4-*di-tert*-butylimidazole-2-thiol in dichloromethane gave deep red and purple solutions of the complexes $[\text{Rh}(\mu\text{-Bu}_2\text{-ImS})(\text{CO})_2]_n$ (**15**) and $[\text{Ir}(\mu\text{-Bu}_2\text{-ImS})(\text{CO})_2]_n$ (**16**), which were isolated as orange and purple microcrystalline solids in good yield. The carbonyl compounds gave satisfactory elemental analysis, and their FAB+ spectra showed the presence of the dinuclear ions. However, the IR spectra in cyclohexane (Figure 6) showed more $\nu(\text{CO})$ bands for the terminal carbonyl groups than expected for a single dinuclear isomer.

The ^1H NMR spectrum of compound **16** in CDCl_3 at RT showed the presence of two main species having equivalent $\mu\text{-Bu}_2\text{-ImS}^-$ ligands. In addition, both species are dynamic and no carbonyl ligands were observed in the $^{13}\text{C}\{^1\text{H}\}$ NMR spectrum as a consequence of scrambling processes involving the carbonyl ligands. The available spectroscopic information suggests that in solution compound **16** exists as an equilibrium (Scheme 7) between the dinuclear $[\text{Ir}(\mu\text{-Bu}_2\text{-ImS})(\text{CO})_2]_2$ ($n = 2$) and mononuclear $[\text{Ir}(\mu\text{-Bu}_2\text{-ImS})(\text{CO})_2]$ ($n = 1$) species, the

(29) Hill, R.; Kelly, B. A.; Kennedy, F. G.; Knox, S. A. R.; Woodward, P. *J. Chem. Soc., Chem. Commun.* **1977**, 434.

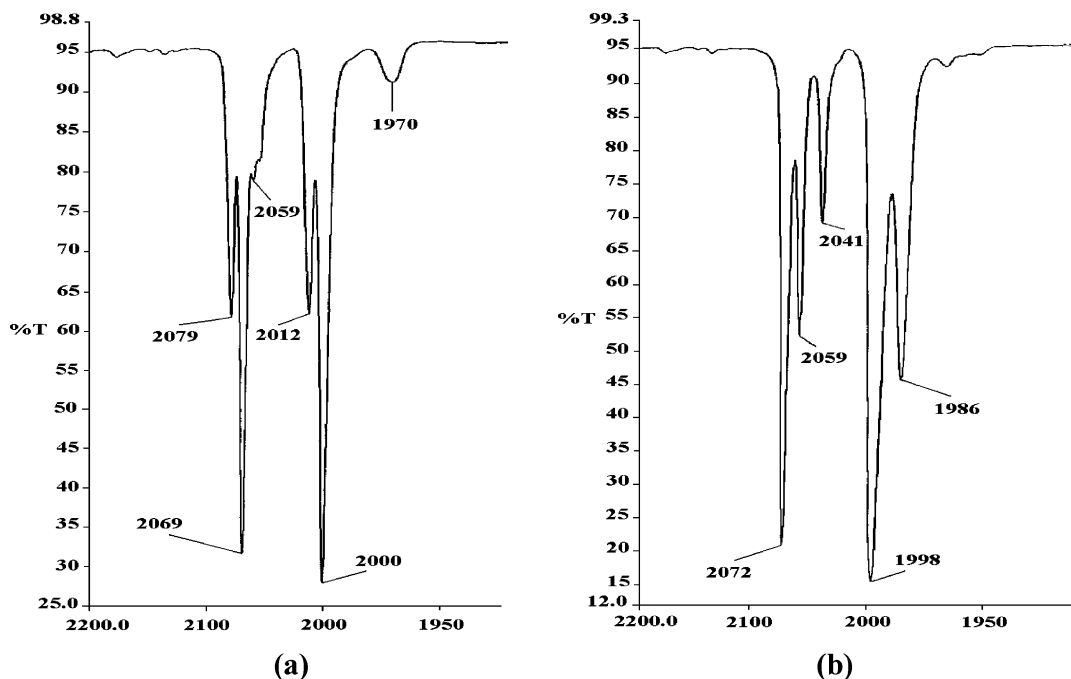


Figure 6. Partial IR spectra of compounds $[M(\mu\text{-}^i\text{Bu}_2\text{-ImS})(\text{CO})_2]_2$ in cyclohexane: (a) $M = \text{Rh}$, **15**; (b) $M = \text{Ir}$, **16**.

former being more abundant ($\approx 75\%$) at room temperature. Thus, the absorptions at $\nu(\text{CO})$ 2072 (s), 2041 (m), and 1998 (s) cm^{-1} in the IR spectrum in cyclohexane (Figure 6b) correspond to the dinuclear species, whereas the bands at $\nu(\text{CO})$ 2059 and 1986 cm^{-1} could be assigned to the mononuclear species. The difference between the last two absorptions (73 cm^{-1}) is typical of mononuclear complexes having two carbonyl ligands in *cis* disposition.^{30,31} The dinuclear species showed the characteristic resonance for the H^5 protons of the $^i\text{Bu}_2\text{-ImS}^-$ ligands at δ 6.51 and isochronous ^iBu groups at 1.48 ppm, whereas the resonances at δ 6.04, 1.58, and 1.23 ppm were assigned to the mononuclear species.

On cooling to -50°C in CDCl_3 the equilibrium is shifted toward the dinuclear species to the extent of 95%, as deduced from the integrals of the H^5 resonances. Interestingly, two sets of equivalent carbonyl ligands were observed in the $^{13}\text{C}\{^1\text{H}\}$ NMR at -50°C , at δ 173.5 and 173.1 ppm, suggesting that the most probable structure of the dinuclear species results from the $\mu\text{-}(1\kappa\text{S},2\kappa\text{N})$ coordination of the bridging ligands with a *cis*-HT disposition (dimer shown in Scheme 7).

The molecular weight of compound $[\text{Rh}(\mu\text{-}^i\text{Bu}_2\text{-ImS})(\text{CO})_2]_n$ (**15**) measured in chloroform (534 vs 740) suggests that an equilibrium similar to that described for compound **16** could be operative. This fact has been corroborated by the spectroscopic data obtained from the IR and NMR, which indicate that the mononuclear species predominates over the dinuclear one. The IR spectrum in cyclohexane (Figure 6a) shows two strong $\nu(\text{CO})$ absorptions at 2069 and 2000 cm^{-1} , which have been assigned to the mononuclear species $[\text{Rh}(\text{Bu}_2\text{-ImS})(\text{CO})_2]$, and three weaker absorptions at $\nu(\text{CO})$ 2079 (s), 2059 (m), and 2012 (s) cm^{-1} , with the usual intensity pattern for a dinuclear $[\text{Rh}(\mu\text{-}^i\text{Bu}_2\text{-ImS})(\text{CO})_2]_2$ (*cis*-HT isomer, Scheme 7) having a face-to-face disposition of both rhodium coordination planes.

The ^1H NMR spectrum of compound **15** is not structurally informative. However, the carbonyl region of the $^{13}\text{C}\{^1\text{H}\}$ NMR spectrum in CDCl_3 at RT showed a doublet at δ 183.9 ppm ($J_{\text{Rh-C}} = 73.4$ Hz) for the mononuclear species $[\text{Rh}(\text{Bu}_2\text{-ImS})(\text{CO})_2]$. As above, the equilibrium is shifted toward the dinuclear species when decreasing the temperature, as indicated by the $^{13}\text{C}\{^1\text{H}\}$ NMR spectrum at -50°C . The spectrum showed the expected two doublet resonances for the *cis*-HT isomer of the dinuclear species at δ 187.0 (d, $J_{\text{Rh-C}} = 64.0$ Hz) and 183.3 (d, $J_{\text{Rh-C}} = 70.3$ Hz) and also a little amount of the mononuclear species. The equivalence of the carbonyl ligands in the mononuclear species results from a dynamic behavior that probably involves the opening and re-forming of the four-membered strained metallaheterocycle via the Rh–N bond. Similar dynamic behavior has been observed in the compounds $[\text{Rh}(\text{SPymMe}_2)(\text{COD})]^{31}$ and $[\text{Rh}(\text{SPymMe}_2)(\text{CO})(\text{PPh}_3)]^{13c}$ containing 4,6-dimethylpyrimidine-2-thiolate ligands.

The carbonylation of the diolefin complexes $[\text{M}(\mu\text{-}^i\text{Bu}_2\text{-ImS})(\text{COD})]_2$ in dichloromethane gave deep colored solutions of the carbonyl complexes $[\text{M}(\mu\text{-}^i\text{Bu}_2\text{-ImS})(\text{CO})_2]_n$ (where $n = 1$ or 2). Further reaction with 2 molar equiv of triphenylphosphine resulted in the evolution of carbon monoxide and the formation of the mononuclear complexes $[\text{Rh}(\text{Bu}_2\text{-ImS})(\text{CO})(\text{PPh}_3)]$ (**17**, Scheme 6) and $[\text{Ir}(\text{Bu}_2\text{-ImS})(\text{CO})(\text{PPh}_3)]$ (**18**), which were isolated as yellow solids in moderate yield. The molecular structure of compound **18** has been determined by an X-ray diffraction analysis and shows a chelating coordination mode ($\kappa^2\text{S,N}$) of the $^i\text{Bu}_2\text{-ImS}^-$ ligand (Figure 7, discussed below).

The spectroscopic data showed that both compounds exist in solution as a single isomer and are compatible with the structure found in the solid state. In particular, the determination of the molecular weights in chloroform indicates that the molecular structure is maintained in solution. The FAB+ spectra of both complexes showed the mononuclear ions $[\text{M}(\text{Bu}_2\text{-ImS})(\text{CO})(\text{PPh}_3)]^+$ at m/z 605 and 694, respectively, although some dinuclear ions were also observed in the spectrum of compound **18**. The $^{31}\text{P}\{^1\text{H}\}$ NMR spectrum of compound **17** in toluene- d_8 shows a slightly broad doublet at δ 49.83 ppm ($J_{\text{Rh-P}} = 156.3$ Hz), which became sharper at -60°C . However, no changes

(30) (a) Teuma, E.; Loy, M.; Le Berre, C.; Etienne, M.; Daran, J.-C.; Kalck, P. *Organometallics* **2003**, *22*, 5661. (b) Elgafi, S.; Field, L. D.; Mecerle, B. A.; Turner, P.; Hambley, T. W. *J. Organomet. Chem.* **1999**, *588*, 69. (c) Crotti, C.; Cenini, S.; Rindone, B.; Tollari, S.; Demartin, F. *Chem. Commun.* **1986**, 784.

(31) Rojas, S.; Fierro, J. L. G.; Fandos, R.; Rodríguez, A.; Terreros, P. *J. Chem. Soc., Dalton Trans.* **2001**, 2316.

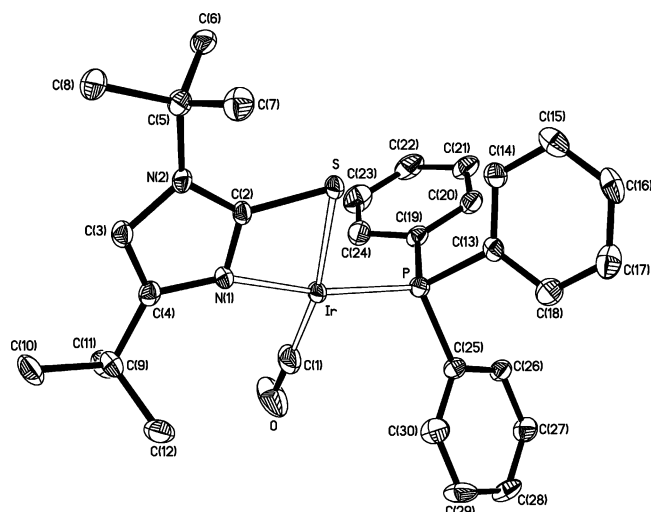


Figure 7. Molecular structure of compound $[\text{Ir}(\mu\text{-}^1\text{Bu}_2\text{-ImS})(\text{CO})(\text{PPh}_3)]$ (**18**).

were observed in the ^1H NMR spectrum between -60 °C and room temperature. The triphenylphosphine ligand in compound **18** was observed as a sharp singlet at δ 19.9 ppm in the $^{31}\text{P}\{^1\text{H}\}$ NMR spectrum in C_6D_6 at RT. Finally, the carbonyl ligand carbon was observed as the expected doublet of doublets at δ 189.8 ppm ($J_{\text{Rh-C}} = 75.3$ Hz, $J_{\text{P-C}} = 19.7$ Hz) (**17**) and as a singlet at δ 176.6 ppm (**18**) in the $^{13}\text{C}\{^1\text{H}\}$ NMR spectra in C_6D_6 at RT. A diagnostic for the $\kappa^2\text{S,N}$ coordination mode of the $^1\text{Bu}_2\text{-ImS}^-$ ligand is the chemical shift of the CS resonance in the $^{13}\text{C}\{^1\text{H}\}$ NMR, which is observed at higher frequency (≈ 158 ppm) than in the dinuclear complexes (≈ 147 ppm). The IR spectra of both compounds in dichloromethane showed a strong $\nu(\text{CO})$ band for the terminal carbonyl ligand at 1968 and 1953 cm^{-1} , respectively.

Molecular Structure of $[\text{Rh}(\mu\text{-}^1\text{Bu}_2\text{-ImS})(\text{COD})]_2$ (13**) and $[\text{Ir}(\mu\text{-}^1\text{Bu}_2\text{-ImS})(\text{CO})(\text{PPh}_3)]$ (**18**).** Good-quality crystals for X-ray diffraction of compound **13** were obtained by slow diffusion of *n*-hexane into a solution of the complex in dichloromethane. The molecular structure is shown in Figure 5, and key bond distances and angles are shown in Table 1. The structure of **13** shows the *syn-endo* disposition of the two thiolates with respect to the folded Rh_2S_2 core. Coordination geometry at both Rh centers is distorted square planar, with clearly acute S–Rh–S angles [$77.09(3)^\circ$ and $77.15(3)^\circ$]. In comparison with the structure of **2**, the M–S–M angles are significantly larger [$92.67(3)^\circ$ and $92.35(3)^\circ$], a reflection of the fact that the M–M bond distance is about 0.5 Å larger [$3.4194(4)$ Å in **13** and $2.9055(8)$ Å in **2**] and that the M_2S_2 core is more open [$139.06(5)^\circ$ fold angle in **13** and $101.02(6)^\circ$ in **2**]. Among related Rh_2S_2 complexes, the metal–metal distance is between extremes, such as the 3.52 Å value cited for $[\text{Rh}(\mu\text{-S-C(R)=NR})(\text{COD})]_2$ ^{22a} and 2.960(1) or 2.955 Å in $[\text{Rh}(\mu\text{-SCH}_2\text{CH}_2\text{CH}_2\text{NMe}_2)(\text{COD})]_2$ ^{24b} and $[\text{Rh}(\mu\text{-SC}_6\text{F}_5)(\text{COD})]_2$ ^{32a}.

Suitable crystals for X-ray diffraction of compound **18** were obtained by slow diffusion of methanol into a solution of the complex in dichloromethane at -15 °C. Key bond distances and angles are shown in Table 4; Figure 7 confirms that the

complex is mononuclear. The sum of the four *cis* intraligand angles is equal to 360.0° within experimental uncertainty, but the individual angles are distorted from idealized values: first, the chelated imidazolethiolate enforces a small S–Ir–N angle [$68.83(9)^\circ$], as expected for such species. In contrast, the largest angle [$103.54(16)^\circ$] is between the Ir–CO bond and the adjacent Ir–N bond, whereas the S–Ir–P angle is rather large [$97.67(4)^\circ$] and the remaining P–Ir–CO angle ideal within experimental uncertainty. The closest analogues for such a species are those derived from $\text{Rh}(\text{CO})(\text{PPh}_3)$ and $\text{Rh}(\text{CO})_2$ fragments and 4,6-dimethylpyrimidine-2-thiolate,^{13c,31} which show very similar distortions in bond angles within a square-planar arrangement.

Discussion

Pyridinethiolate Complexes of $^1\text{Bu-PyS}$. The dinuclear complexes $[\text{M}(\mu\text{-}^1\text{Bu-PyS})(\text{L}_2)]_2$ (M = Rh, Ir) display an open-book structure resulting from the thiolate $\mu\text{-}(1:2\kappa^2\text{S})$ coordination mode of the $^1\text{Bu-PyS}^-$ ligands irrespective of the steric and electronic properties of the auxiliary ligands. The only influence of the terminal ligands appears to be related with the spatial disposition of the thiolate bridges. Ab initio theoretical studies on edge-sharing dinuclear d^8 complexes with thiolate ligands³³ indicate that the bent structure is more favorable for rhodium and iridium complexes as a consequence of the tendency of the metals to form M–M contacts. The possible conformations of the bridging ligands (*syn-exo*, *syn-endo*, and *anti*) seem to be determined by the interplay of several factors including the existence of weak metal–metal bonding, the increased steric repulsion between terminal ligands upon bending, the steric repulsion between the substituents at the bridging atoms, and the hydrogen-bonding interactions involving the terminal ligands and the substituents at the bridges.

The complexes $[\text{M}(\mu\text{-}^1\text{Bu-PyS})(\text{COD})]_2$ (M = Rh, **1**; Ir, **2**) present a *syn-endo* conformation of the thiolato ligands. Interestingly, a number of dinuclear rhodium and iridium complexes containing cyclooctadiene as bidentate terminal ligands and terminal thiolate ligands as bridges display the *syn-endo* conformation in the solid state^{22a,24b,32c,d} and have a dynamic behavior similar to that found in complexes **1** and **2**.^{32c,d} Similarly, the *syn* disposition is also the preferred conformation for thiolate-bridged complexes with four terminal carbonyl ligands and the *endo* conformer is usually found in the solid state (in accordance with the theoretical calculations).³⁴ It is noticeable that the spectroscopic data for the tetracarbonyl complexes $[\text{M}(\mu\text{-}^1\text{Bu-PyS})(\text{CO})_2]_2$ (M = Rh, **3**; Ir, **4**) are also in agreement with a *syn* conformation of the $^1\text{Bu-PyS}^-$ ligands. In contrast, the complexes $[\text{M}(\mu\text{-}^1\text{Bu-PyS})(\text{CO})(\text{PPh}_3)]_2$ (M = Rh, **5**; Ir, **6**), containing two bulky triphenylphosphine ligands arranged in a *cis* disposition, display an *anti* conformation with the *endo* substituent at the side of the molecule with the small carbonyl ligands, as is generally found in related complexes containing both monodentate^{25a–c} and bridging diphosphine³⁵ ligands.

The results described above contrast with the ability of the related parent compound pyridine-2-thiolate to bridge rhodium or iridium centers in dinuclear complexes through the N and S atoms. For example, the complexes $[\text{Rh}(\mu\text{-SPy})(\text{COD})]_2$, $[\text{Rh}(\mu\text{-SPy})(\text{CO})_2]_2$, and $[\text{Rh}(\mu\text{-SPy})(\text{CO})(\text{PPh}_3)]_2$ ^{13b–d} all have a *cis*-

(32) (a) Cruz-Garriz, D.; Rodríguez, B.; Torrens, H.; Leal, J. *Transition Met. Chem. (Dordrecht)* **1984**, *9*, 284. (b) Cruz-Garriz, D.; Garcia-Alejandro, J.; Torrens, H.; Alvarez, C.; Toscano, R. A.; Poilblanc, R.; Thorez, A. *Transition Met. Chem. (Dordrecht)* **1991**, *16*, 130. (c) Fandos, R.; Martínez-Ripoll, M.; Otero, A.; Ruiz, M. J.; Rodríguez, A.; Terreros, P. *Organometallics* **1998**, *17*, 1465. (d) Wark, T. A.; Stephan, D. W. *Can. J. Chem.* **1990**, *68*, 565.

(33) Aullón, G.; Ujaque, G.; Lledós, A.; Alvarez, S. *Chem. Eur. J.* **1999**, *5*, 1391.

(34) (a) Pursiainen, J.; Teppana, T.; Rossi, S.; Pakkanen, T. A. *Acta Chem. Scand.* **1993**, *47*, 416. (b) Bonet, J. J.; de Mountazon, D.; Poilblanc, R.; Galy, J. *Acta Crystallogr. Sect. B* **1979**, *35*, 832.

HT dinuclear structure resulting from the thionate coordination mode μ -(1 κ S,2 κ N) of both SPy⁻ ligands. Thus, the presence of a bulky *tert*-butyl substituent at position 6 of the pyridine-2-thionate structure reduces the ability of the pyridine nitrogen atom to coordinate, and as a consequence, the 'Bu-PyS⁻ ligand behaves as a normal thiolate ligand. It would be of interest to determine the minimum size of a substituent needed to give this result. However, we note that in related systems neither a methyl nor a chloro substituent is sufficient, because the related pyridonate dinuclear complexes [M(μ -OPy)(CO)₂]₂,³⁶ [M(μ -OMePy)(COD)]₂ (M = Rh, Ir)²³ and [Rh(μ -OCIPy)(nbd)]₂³⁷ (OPy⁻ = 2-pyridonate, OMePy⁻ = 6-methyl-2-pyridonate, OCIPy⁻ = 6-chloro-2-pyridonate) all display structures with staggered face-to-face d⁸-ML₂ environments derived from the μ -(1 κ O,2 κ N) coordination mode of the pyridonate ligands, irrespective of the substitution at the position *ortho* to the pyridine nitrogen.

Imidazolethiolate Complexes from Me-'Bu-ImS and 'Bu₂-ImS. In contrast to what was seen using the 6-*tert*-butylpyridine-2-thiolate ligand, the imidazole-2-thiolate derivatives can act as bidentate bridges through the N and S heteroatoms even in the presence of bulky substituents on the heterocycle. In fact, from literature structures of 1-methyl-imidazole-2-thiolate complexes, coordination through only the sulfur atom appears to be rare, whether in mononuclear complexes or in dinuclear species as bridging [μ -(1:2 κ^2 S)] ligands.¹⁴ Instead, the more usual coordination modes of this ligand are μ -(1 κ S,2 κ N),¹⁵ μ -(1 κ N,1:2 κ S),¹⁶ and (κ^2 S,N).¹⁷ In general, three factors may explain the higher propensity of the imidazole derivatives to act as bidentate ligands. First, imidazoles are more basic than pyridines, by about 2 pK_a units.³⁸ Second, in the smaller, five-membered ring, the steric influence of the *tert*-butyl group on the adjacent N-heterocyclic donor atom should be reduced. Finally, a five-membered heterocycle ring results in significantly larger N–C–S bond angles that can produce more open dinuclear structures, resulting in less steric interference between the bridging and terminal ligands. In this context, we note that the rhodium and iridium coordination chemistry of the five-membered heterocyclic ligands benzothiazole-2-thiolate,^{13b,27,39} 2-mercaptothiazolinate,^{28a,40} and benzimidazole-2-thiolate⁴¹ have been studied in detail. However, neither rhodium nor iridium

complexes of the related ligands imidazole-2-thiolate and 1-methylimidazole-2-thiolate have been structurally characterized.

It is worthy of notice that dinuclear complexes are usually obtained with the 1-methyl-4-*tert*-butylimidazole-2-thiolate ligand, although the interplay between the bulky *tert*-butyl group at the 4 position and the steric properties of the auxiliary ligands determines the coordination mode and the relative disposition of the bridging ligands. However, the second *tert*-butyl group at the N atom of the heterocycle in the ligand 1,4-di-*tert*-butylimidazole-2-thiolate changes both the coordination mode of the ligands and the nuclearity of the complexes.

When the auxiliary ligands are 1,5-cyclooctadiene, the dinuclear complexes are dynamic, displaying at the stopped-exchange limit a μ -(1:2 κ^2 S)(1 κ S,2 κ N) coordination of the bridging ligands as in the complexes [M(μ -Me-'Bu-ImS)(COD)]₂ (M = Rh, **7**; Ir, **8**) and [Ir(μ -'Bu₂-ImS)(COD)]₂ (**14**). Moreover, the change in the coordination mode of the ligands from μ -(1 κ S,2 κ N) to μ -(1:2 κ^2 S) appears to be responsible for the fluxional behavior in solution. Interestingly, as the bulkiness of the bridging ligand is increased, the difficulties for the μ -(1 κ S,2 κ N) coordination result in the μ -(1:2 κ^2 S) coordination of both thiolates, as in the dinuclear complexes **13** and **14** (at room temperature), which display a typical bis-thiolate dinuclear structure with relative dispositions *syn-endo* and *anti*, respectively. Moreover, the dinuclear complex [Rh(μ -'Bu₂-ImS)(COD)]₂ (**13**) appears to be in equilibrium with the mononuclear compound [Rh('Bu₂-ImS)(COD)] at room temperature, a conversion perhaps driven by release of strain.

The smaller carbonyl ligands facilitate the μ -(1 κ S,2 κ N) coordination mode of the bridging ligands, as demonstrated in the dinuclear complexes [M(μ -Me-'Bu-ImS)(CO)₂]₂ (M = Rh, **9**; Ir, **10**). Interestingly, the complexes are obtained exclusively as the *cis*-HT isomer since with this disposition the *tert*-butyl groups are placed further apart in the dinuclear structure. Related tetracarbonyl complexes such as [M(μ -OPy)(CO)₂]₂ (M = Rh, Ir),³⁶ [Ir(μ -SPy)(CO)₂]₂,⁴² and [Rh(μ -bzta)(CO)₂]₂^{13b} exist in solution as the *cis*-HH and *cis*-HT isomers, generally in equilibrium, although only one isomer has been found in the solid state. However, the complexes [Rh(μ -SPy)(CO)₂]₂^{13d} and [Ir(μ -bzta)(CO)₂]₂⁴³ are dynamic but exist as a single isomer in solution at low temperature.

In contrast, the complexes [M(μ -'Bu₂-ImS)(CO)₂]_n (M = Rh, **15**; Ir, **16**), containing the bulkier 1,4-di-*tert*-butylimidazole-2-thiolate bridging ligands, exist in solution as an equilibrium between dinuclear (*n* = 2) and mononuclear (*n* = 1) complexes, whose composition depends on the metal center (Rh or Ir) and the temperature. Thus, the mononuclear [Rh('Bu₂-ImS)(CO)₂] and the dinuclear [Ir(μ -'Bu₂-ImS)(CO)₂]₂ species are predominant at room temperature; however, in both cases the equilibrium is shifted to the dinuclear species as the temperature decreased. An analogous equilibrium between di- and mononuclear complexes in palladium chemistry has been observed by Jensen et al. in the dynamic dinuclear complexes [Pd(μ -PyS)Cl(PMe₃)₂]₂,⁴⁴ [Pd(μ -SPym)Cl(PMe₃)₂] (SPym⁻ = pyrimidine-2-thiolate), and [Pd(μ -SPymMe)Cl(PMe₃)₂] (SPymMe⁻ = 4-methylpyrimidine-2-thiolate) but not in [Pd(μ -MeImS)Cl(PMe₃)₂] (MeImS⁻ = 1-methylimidazole-2-thiolate), which is dinuclear and static in solution.^{15d}

(35) (a) Choukroun, R.; Dahan, F.; Gervais, D.; Rifai, C. *Organometallics* **1990**, *9*, 1982. (b) Kalck, P.; Randrianalimanana, C.; Ridmy, M.; Thorez, A.; tom Dieck, H.; Ehlers, J. *New J. Chem.* **1988**, *12*, 679.

(36) (a) Tejel, C.; Ciriano, M. A.; Villarroya, B. E.; Gelpi, R.; López, J. A.; Lahoz, F. J.; Oro, L. A. *Angew. Chem. Int. Ed.* **2001**, *40*, 4084. (b) Ciriano, M. A.; Villarroya, B. E.; Oro, L. A.; Apreda, C.; Foces-Foces, F. H.; Cano, J. J. *Organomet. Chem.* **1989**, *366*, 377.

(37) Boyd, D. C.; Szalapski, R.; Mann, K. R. *Organometallics* **1989**, *8*, 790.

(38) Perrin, D. D. *Dissociation Constants of Organic Bases in Aqueous Solution*; Butterworth: London, 1965.

(39) (a) Ciriano, M. A.; Pérez-Torrente, J. J.; Oro, L. A.; Tiripicchio, A.; Tiripicchio-Camellini, M.; López, J. A.; Lanfranchi, M. *Organometallics* **1995**, *14*, 4764. (b) Ciriano, M. A.; Pérez-Torrente, J. J.; Oro, L. A.; Tiripicchio, A. *J. Organomet. Chem.* **1994**, *469*, C31. (c) Ciriano, M. A.; Pérez-Torrente, J. J.; Oro, L. A.; Lahoz, F. J. *Inorg. Chem.* **1992**, *31*, 969. (d) Ciriano, M. A.; Pérez-Torrente, J. J.; Oro, L. A.; Tiripicchio, A.; Tiripicchio-Camellini, M.; J. *Chem. Soc., Dalton Trans.* **1991**, 255. (e) Ciriano, M. A.; Pérez-Torrente, J. J.; Oro, L. A.; Viguri, F.; Tiripicchio, A.; Tiripicchio-Camellini, M.; Lahoz, F. J. *J. Chem. Soc., Dalton Trans.* **1990**, 1493. (f) Ciriano, M. A.; Oro, L. A.; Pérez-Torrente, J. J.; Tiripicchio, A.; Tiripicchio-Camellini, M. *J. Chem. Soc., Chem. Commun.* **1986**, 1737.

(40) Slielisch, T.; Cowie, M. *Organometallics* **1988**, *7*, 707.

(41) (a) Tejel, C.; Villarroya, B. E.; Ciriano, M. A.; Edwards, A. J.; Lahoz, F. J.; Oro, L. A.; Lanfranchi, M.; Tiripicchio, A.; Tiripicchio-Camellini, M. *Inorg. Chem.* **1998**, *37*, 3954. (b) Tejel, C.; Villarroya, B. E.; Ciriano, M. A.; Oro, L. A.; Lanfranchi, M.; Tiripicchio, A.; Tiripicchio-Camellini, M. *Inorg. Chem.* **1996**, *35*, 4360.

(42) Ciriano, M. A.; Viguri, F.; Oro, L. A.; Tiripicchio, A.; Tiripicchio-Camellini, M. *Angew. Chem., Int. Ed. Engl.* **1988**, *28*, 444.

(43) Ciriano, M. A.; Sebastián, S.; Oro, L. A.; Tiripicchio, A.; Tiripicchio-Camellini, M. *Angew. Chem., Int. Ed. Engl.* **1987**, *27*, 402.

(44) Yamamoto, J. H.; Yoshida, W.; Jensen, C. M. *Inorg. Chem.* **1991**, *30*, 1353.

The combination of the bulky 1,4-di-*tert*-butylimidazole-2-thiolate and triphenylphosphine ligands results in the formation of the mononuclear complexes $[M(^t\text{Bu}_2\text{-ImS})(\text{CO})(\text{PPh}_3)]$ ($M = \text{Rh}$, **17**; Ir , **18**), which exhibit a chelating coordination mode ($\kappa^2\text{S,N}$) of the $^t\text{Bu}_2\text{-ImS}^-$ ligand. Interestingly, the structure may also be determined by steric factors, as the PPh_3 ligand is coordinated *trans* to the N atom in the four-membered metallacycle in order to avoid steric repulsions with the ^tBu at position 4. It is worth noting that the mononuclear complexes $[\text{Rh}(^t\text{Bu}_2\text{-ImS})(\text{COD})]$ and $[\text{M}(^t\text{Bu}_2\text{-ImS})(\text{CO})(\text{PPh}_3)]$ ($M = \text{Rh}$, Ir) are static, but the carbonyl complexes $[\text{M}(^t\text{Bu}_2\text{-ImS})(\text{CO})_2]$ are dynamic. It may be that the equivalence of the carbonyl ligands is attained through the intermediary three-coordinated species resulting from the decoordination of the nitrogen, which is facilitated by both the strong labilizing effect of the strong π -acceptor carbonyl ligands and the strain of the four-membered metallacycle.

Therefore, the introduction of two *t*-Bu groups on the imidazole-2-thiolate framework induces the formation of mononuclear compounds by destabilization of the dinuclear structure by steric and electronic means. In sharp contrast, the *cis*-HT dinuclear structure of the complexes $[\text{M}(\mu\text{-Me-}^t\text{Bu-ImS})(\text{CO})(\text{PPh}_3)]_2$ ($M = \text{Rh}$, **11**; Ir , **12**) results from the $\mu\text{-}(1\kappa\text{S},2\kappa\text{N})$ coordination of both 1-methyl-4-*tert*-butylimidazole-2-thiolate ligands. These results point out that the steric influence of the N- ^tBu substituent is greater than that of the N-Me, which, in turn, seems to be responsible for the nuclearity of the complexes.

The steric influence of the bridging ligands on their coordination mode has been observed in dinuclear *cis*-HT complexes with tridentate 1,8-naphthyridin-2-onate ligands. Thus, the coordination of the ligands in the complex $[\text{Rh}(\mu\text{-Onapy})(\text{CO})_2]_2$ is $\mu\text{-}(1\kappa\text{N},2\kappa\text{N})$ but $\mu\text{-}(1\kappa\text{N},2\kappa\text{O})$ in the complex $[\text{Rh}(\mu\text{-OMePhnapy})(\text{CO})_2]_2$ ($\text{OMePhnapy}^- = 5\text{-methyl-7-phenyl-1,8-naphthyridin-2-onate}$) as an effect of the bulky phenyl rings.⁴⁵ On the other hand, the structural influence of the terminal ligands has been observed in the complexes $[\text{Rh}(\mu\text{-OMe}_2\text{napy})(\text{COD})]_2$ and $[\text{Rh}_2(\mu\text{-OMe}_2\text{napy})_2(\text{CO})_2(\text{COD})]$, which have $\mu\text{-}(1\kappa\text{N},2\kappa\text{O})$ -coordinated bridging ligands and display *cis*-HT and *cis*-HH structures, respectively.⁴⁶

Conclusions

The profound steric effect of a bulky *tert*-butyl group adjacent to nitrogen in $^t\text{Bu-PyS}$ makes it coordinate like a normal thiolate such as PhS : no evidence for metal–nitrogen interaction was seen. In contrast, despite the presence of a *tert*-butyl group in a similar position on the two imidazole ligands, complexes with metal–nitrogen coordination were isolated. This shows a stronger coordination ability of imidazole, as evidenced not only in two bridging coordination modes $[\mu\text{-}(1\kappa\text{S},2\kappa\text{N})$ and $\mu\text{-}(1:2\kappa^2\text{S})$ in **7**] but also in a mononuclear species as a chelating ligand $[\kappa^2\text{S,N}$ in **18**]. Among imidazolethiolate complexes, changing the steric demand of the nonbasic ring nitrogen ($\text{Me-}^t\text{Bu-ImS}$ vs $^t\text{Bu}_2\text{-ImS}$) partially controls access to the sulfur atom and hence modifies the capacity of the thiolate to bridge metals.

Experimental Section

General Procedures. All manipulations were performed under dry argon atmosphere using Schlenk techniques. Solvents were dried by standard methods and distilled under argon immediately prior

to use.⁴⁷ The complexes $[\text{Rh}(\mu\text{-Cl})(\text{COD})]_2$,⁴⁸ $[\text{Ir}(\mu\text{-Cl})(\text{COD})]_2$,⁴⁸ $[\text{Ir}(\mu\text{-OMe})(\text{COD})]_2$,⁴⁹ $[\text{Rh}(\mu\text{-OMe})(\text{COD})]_2$,⁴⁹ $[\text{Rh}(\text{acac})(\text{CO})]_2$,⁵⁰ $[\text{Rh}(\text{acac})(\text{CO})(\text{PPh}_3)]$,⁵⁰ $[\text{Ir}(\text{acac})(\text{CO})]_2$,⁵¹ $[\text{Ir}(\text{acac})(\text{CO})(\text{PPh}_3)]$,⁵¹ and precursor 6-*tert*-butyl-2-pyridinone¹⁸ were prepared by known procedures. 1-Methyl-*tert*-butylimidazole-2-thiol was made as recently reported.¹⁹ NMR spectra were recorded at 300, 400, or 500 MHz with Varian and Bruker spectrometers at variable temperature. ^1H and $^{13}\text{C}\{^1\text{H}\}$ NMR chemical shifts are reported in ppm downfield from tetramethylsilane and referenced to residual solvent resonances [^1H NMR: 7.25 for CHCl_3 in CDCl_3 , 5.32 for CHDCl_2 in CD_2Cl_2 , 2.09 for $\text{C}_6\text{D}_5\text{CHD}_2$ in toluene- d_8 , and 7.15 for C_6HD_5 in C_6D_6 . $^{13}\text{C}\{^1\text{H}\}$ NMR: 77.23 for CDCl_3 , 54.00 for CD_2Cl_2 , and 128.39 for C_6D_6], where ^1H NMR signals are given followed by multiplicity, coupling constants J in hertz, and integration in parentheses. For complex coupling patterns listed, e.g., for (dt, $J = 3.2, 7.9, 1\text{H}$), the doublet exhibits a 3.2 Hz coupling constant. $^{31}\text{P}\{^1\text{H}\}$ NMR chemical shifts were measured relative to H_3PO_4 (85%). Molecular weights were determined in chloroform solutions on a Knauer vapor pressure osmometer (isopiestic method). Carbon, hydrogen, nitrogen, and sulfur analyses were carried out in a Perkin-Elmer 2400 CHNS/O analyzer. IR spectra were obtained in solution held in NaCl cells using an FT-IR spectrophotometer (either Bruker Equinox 55 or Perkin-Elmer Spectrum One). MS data were recorded on a VG Autospec double-focusing mass spectrometer operating in the positive mode. Ions were produced with a Cs^+ gun at ca. 30 kV, and 3-nitrobenzyl alcohol (NBA) was used as the matrix.

Synthesis of 1,4-Di-*tert*-butylimidazole-2-thiol. To a solution of 1-bromo-3,3-dimethyl-2-butanone (20.0 g, 112 mmol) in THF (250 mL) was added *tert*-butylamine (24.5 g, 335 mmol) in one portion, and the mixture was heated under reflux for 1 day. After workup with water and diethyl ether, crude 1-(*tert*-butylamino)-3,3-dimethylbutan-2-one (15.2 g) remained. ^1H NMR (CDCl_3 , 199.97 MHz, 25 °C): δ 3.64 (s, 2 H, CH_2), 1.17 (s, 9 H, CH_3 , N- ^tBu), 1.10 ppm (s, 9 H, CH_3 , ^tBu). Crude 1-(*tert*-butylamino)-3,3-dimethylbutan-2-one in ethanol (100 mL) and a solution of KSCN (9.95 g, 103 mmol) in 2 N HCl (3.5 mL) were heated under reflux overnight. The room-temperature mixture was diluted with water (250 mL) and placed in the freezer to complete precipitation of 1,4-di-*tert*-butylimidazole-2-thiol (9.58 g, 51%). Mp: 286.7–292.3 °C (dec), raised to 288.0–291.0 °C by rinsing of crystals with ethyl acetate and subsequent recrystallization from THF and hexanes. ^1H NMR (CDCl_3 , 300.08 MHz, 30 °C): δ 10.4 (br s, 1 H), 6.42 (d, $J = 1.8$ Hz, 1 H), 1.81 (s, 9 H), 1.25 ppm (s, 9 H). $^{13}\text{C}\{^1\text{H}\}$ NMR (CDCl_3 , 50.2 MHz, 30 °C): δ 158.4, 137.0, 109.2, 58.3, 30.2, 29.3, 28.2. Anal. Calcd for $\text{C}_{11}\text{H}_{20}\text{N}_2\text{S}$ (212.35): C, 62.22; H, 9.49; N, 13.19. Found: C, 62.24; H, 9.35; N, 13.24.

Synthesis of 6-*tert*-Butylpyridine-2-thiol. Argon was bubbled through a solution of 6-*tert*-butyl-2-pyridinone (4.00 g, 26.5 mmol) in toluene (100 mL) for 10 min. Lawesson's reagent (5.350 g, 3.22 mol) was then added, and the reaction mixture was heated to reflux for 22 h. The mixture was cooled at room temperature, and water (100 mL) was added. After 1 h of stirring, phases were separated and the aqueous phase was extracted with diethyl ether (4×30 mL). The organic fractions were combined, washed with water (4×50 mL), dried over magnesium sulfate, and filtered. After removing the solvent under vacuum, the yellow crude solid was

(47) (a) Shriver, D. F. *The Manipulation of Air-sensitive Compounds*; McGraw-Hill: New York, 1969. (b) Armarego, W. L. F.; Perrin, D. D. *Purification of Laboratory Chemicals*, 4th ed.; Butterworth-Heinemann: Oxford, 1996.

(48) Giordano, G.; Crabtree, R. H. *Inorg. Synth.* **1979**, *19*, 218.

(49) Usón, R.; Oro, L. A.; Cabeza, J. *Inorg. Synth.* **1985**, *23*, 126.

(50) (a) Hernández-Gruel, M. A. F.; Pérez-Torrente, J. J.; Ciriano, M. A.; Oro, L. A. *Inorg. Synth.* **2004**, *34*, 127. (b) Bonati, F.; Wilkinson, G. J. *Chem. Soc.* **1964**, 3156.

(51) Pitt, C. G.; Monteith, L. K.; Ballard, L. F.; Collman, J. P.; Morrow, J. C.; Roper, W. R.; Ulk, D. J. *Am. Chem. Soc.* **1996**, *88*, 4286.

(45) Minteert, M.; Sheldrick, W. S. *Inorg. Chim. Acta* **1997**, *254*, 93.

(46) Villarroya, B. E.; Oro, L. A.; Lahoz, F. J.; Edwards, A. J.; Ciriano, M. A.; Alonso, P. J.; Tiripicchio, A.; Tiripicchio-Camellini, M. *Inorg. Chim. Acta* **1996**, *250*, 241.

purified by column chromatography on silica gel by using CH₂-Cl₂/petroleum ether (1:1) and CH₂Cl₂/MeOH (99:1) solvent systems to yield pure 6-*tert*-butylpyridine-2-thiol (3.938 g, 89%). ¹H NMR (CDCl₃, 300.08 MHz, 30 °C): δ 10.54 (br s, 1 H), 7.38 (d, J = 8.7 Hz, 1 H), 7.27 (t, J = 7.2 Hz, 1 H), 6.57 (d, J = 7.2 Hz, 2 H), 1.33 (s, 9 H). ¹³C{¹H} NMR (CDCl₃, 125.7 MHz, 30 °C): δ 158.9, 138.1, 131.1, 109.3, 35.2, 29.3. Anal. Calcd for C₉H₁₃NS (167.27): C, 64.62; H, 7.83; N, 8.37. Found: C, 65.02; H, 7.87; N, 8.01.

Representative Procedure for the Synthesis of [M(HetS)(COD)]_n Complexes. Synthesis of [Rh(μ-^tBu-PyS)(COD)]₂ (1). [Rh(μ-OMe)(COD)]₂ (0.200 g, 0.413 mmol) and 6-*tert*-butylpyridine-2-thiol (0.138 g, 0.826 mmol) were dissolved in dry CH₂Cl₂ (4 mL) to give immediately an orange solution. The mixture was stirred 3.5 h at room temperature and concentrated under vacuum to 1–2 mL. Addition of cold MeOH (3 mL) to the concentrated solution gave the product as a yellow microcrystalline solid, which was filtered off, washed with cold MeOH (2 × 5 mL), and vacuum-dried (0.261 g, 84%). ¹H NMR (CD₂Cl₂, 300.13 MHz, 25 °C): δ 7.38 (t, J = 7.7 Hz, 2 H, H⁴), 7.16 (d, J = 7.5 Hz, 2 H, H³), 7.04 (d, J = 7.6 Hz, 2 H, H⁵), 4.84 (br s, 8 H, =CH, COD), 2.42 (br m, 8 H, CH₂, COD), 1.96 (br m, 8 H, CH₂, COD), 1.32 (s, 18 H, CH₃, ^tBu). ¹H NMR (CD₂Cl₂, 300.13 MHz, -70 °C): δ 7.34 (t, J = 7.7 Hz, 2 H, H⁴), 7.06 (d, J = 7.6 Hz, 2 H, H³), 6.99 (d, J = 7.7 Hz, 2 H, H⁵), 4.98 (br s, 4 H, =CH, COD), 4.43 (br s, 4 H, =CH, COD), 2.33 (br m, 8 H, CH₂, COD), 1.87 (br m, 8 H, CH₂, COD), 1.20 (s, 18 H, CH₃, ^tBu). ¹³C{¹H} NMR (CD₂Cl₂, 75.46 MHz, 25 °C): δ 169.9 (SC), 158.9 (C⁶), 136.3 (C⁵), 126.9 (C⁴), 116.4 (C³), 80.3 (d, J_{C-Rh} = 11.9 Hz, =CH, COD), 38.2 (C, ^tBu), 31.6 (CH₂, COD), 30.2 (CH₃, ^tBu). ¹³C{¹H} APT NMR (CD₂Cl₂, 75.47 MHz, -70 °C): δ 168.7 (SC), 157.3 (C⁶), 135.6 (C⁵), 125.7 (C⁴), 115.5 (C³), 81.3 (br s, =CH, COD), 77.9 (br s, =CH, COD), 37.3 (C, ^tBu), 30.8 (CH₂, COD), 29.2 (CH₃, ^tBu). MW: found 717.6 (calcd 754.69). MS [FAB⁺ m/z (%): 755 (55) [MH]⁺, 646 (100) [M⁺ - COD]. Anal. Calcd for C₃₄H₄₈N₂S₂Rh₂ (754.69): C, 54.11; H, 6.41; N, 3.71; S, 8.50. Found: C, 54.01; H, 5.92; N, 3.42; S, 8.60.

Synthesis of [Ir(μ-^tBu-PyS)(COD)]₂ (2). Following the general procedure, [Ir(μ-OMe)(COD)]₂ (0.273 g, 0.413 mmol) and 6-*tert*-butylpyridine-2-thiol (0.138 g, 0.826 mmol) were used to prepare **2** (0.328 g, 86%). ¹H NMR (CDCl₃, 300.13 MHz, 22 °C): δ 7.41 (t, J = 7.8 Hz, 2 H, H⁴), 7.20 (d, J = 7.7 Hz, 2 H, H³), 7.06 (d, J = 7.8 Hz, 2 H, H⁵), 4.56 (br s, 8 H, =CH, COD), 2.17 (br m, 8 H, CH₂, COD), 1.70 (br m, 8 H, CH₂, COD), 1.30 (s, 18 H, CH₃, ^tBu). ¹H NMR (CDCl₃, 300.13 MHz, -55 °C): δ 7.43 (t, J = 7.8 Hz, 2 H, H⁴), 7.17 (d, J = 7.7 Hz, 2 H, H³), 7.05 (d, J = 7.7 Hz, 2 H, H⁵), 4.74 (br s, 4 H, =CH, COD), 4.26 (br s, 4 H, =CH, COD), 2.21 (br s, 4 H, CH₂, COD), 2.06 (br s, 4 H, CH₂, COD), 1.81 (br m, 4 H, CH₂, COD), 1.54 (br m, 4 H, CH₂, COD), 1.26 (s, 18 H, CH₃, ^tBu). ¹³C{¹H} APT NMR (CDCl₃, 100.63 MHz, 25 °C): δ 169.6 (SC), 153.4 (C⁶), 136.2 (C⁵), 126.6 (C⁴), 117.0 (C³), 65.1 (=CH, COD), 38.0 (C, ^tBu), 32.1 (CH₂, COD), 30.1 (CH₃, ^tBu). ¹³C{¹H} APT NMR (CDCl₃, 75.47 MHz, -55 °C): δ 169.2 (SC), 152.7 (C⁶), 136.2 (C⁵), 126.2 (C⁴), 116.8 (C³), 66.5 (=CH, COD), 64.2 (=CH, COD), 37.8 (C, ^tBu), 32.1 (CH₂, COD), 31.8 (CH₂, COD), 29.8 (CH₃, ^tBu). MW: found 934.4 (calcd 933.3). MS [FAB⁺ m/z (%): 933 (36) [M]⁺, 824 (18) [M⁺ - COD]. Anal. Calcd for C₃₄H₄₈N₂S₂Ir₂ (933.32): C, 43.75; H, 5.18; N, 3.00; S, 6.87. Found: C, 43.45; H, 4.95; N, 2.92; S, 6.33.

Synthesis of [Rh(μ-Me-^tBu-ImS)(COD)]₂ (7). Following the general procedure, [Rh(μ-OMe)(COD)]₂ (0.200 g, 0.413 mmol) and 1-methyl-4-*tert*-butylimidazole-2-thiol (0.140 g, 0.826 mmol) were used to prepare **7** (0.258 g, 82%). ¹H NMR (CD₂Cl₂, 400.16 MHz, 25 °C): δ 6.50 (s, 2 H, H⁵), 4.59 (br s, 8 H, =CH, COD), 3.45 (s, 6 H, N-CH₃), 2.47 (br m, 8 H, CH₂, COD), 1.93 (br m, 8 H, CH₂, COD), 1.28 (s, 18 H, CH₃, ^tBu). ¹H NMR (CD₂Cl₂, 300.13 MHz, -95 °C): δ 6.51 (s, 1 H, H⁵), 6.45 (s, 1 H, H⁵), 5.12 (br s, 1 H, =CH, COD), 4.74 (br m, 3 H, =CH, COD), 4.09 (br m, 1 H, =

CH, COD), 3.83 (br s, 1 H, =CH, COD), 3.58 (br m, 1 H, =CH, COD), 3.29 (s, 3 H, N-CH₃), 3.27 (s, 3 H, N-CH₃), 3.06 (br s, 1 H, =CH, COD), 2.74 (br s, 2 H, >CH₂, COD), 2.49 (br s, 1 H, >CH₂, COD), 2.17–1.88 (br m, 7 H, >CH₂, COD), 1.51 (br s, 11 H, CH₂, COD, and CH₃, ^tBu), 1.04 (br s, 9 H, CH₃, ^tBu). ¹³C{¹H} NMR (CD₂Cl₂, 75.46 MHz, 25 °C): δ 151.2 (SC), 142.6 (C⁴), 116.2 (C⁵), 81.2 (d, J_{C-Rh} = 11.92 Hz, =CH, COD), 33.9 (N-CH₃), 32.3 (C, ^tBu), 31.6 (CH₂, COD), 30.4 (CH₃, ^tBu). ¹³C{¹H} APT NMR (CD₂Cl₂, 75.47 MHz, -95 °C): δ 149.6 (SC), 149.3 (SC), 146.5 (C⁴), 140.3 (C⁴), 33.9 (N-CH₃), 33.1 (N-CH₃), 31.6 (CH₂, COD), 31.0 (C, ^tBu), 30.5 (CH₃, ^tBu), 28.6 (CH₃, ^tBu). MS [FAB⁺ m/z (%): 760 (20) [M]⁺, 652 (31) [M⁺ - COD]. Anal. Calcd for C₃₂H₅₀N₄S₂Rh₂ (760.71): C, 50.52; H, 6.63; N, 7.37; S, 8.43. Found: C, 50.25; H, 6.53; N, 7.32; S, 8.66.

Synthesis of [Ir(μ-Me-^tBu-ImS)(COD)]₂ (8). Following the general procedure, [Ir(μ-OMe)(COD)]₂ (0.273 g, 0.413 mmol) and 1-methyl-4-*tert*-butylimidazole-2-thiol (0.140 g, 0.826 mmol) were used to prepare **8** (0.352 g, 91%). ¹H NMR (toluene-*d*₈, 300.12 MHz, 70 °C): δ 6.06 (s, 2 H, H⁵), 4.46 (br s, 8 H, =CH, COD), 2.94 (br s, 6 H, N-CH₃), 2.36 (br s, 8 H, CH₂, COD), 1.66 (br s, 8 H, CH₂, COD), 1.40 (br s, 24 H, CH₃, ^tBu). ¹H NMR (toluene-*d*₈, 300.12 MHz, 25 °C), selected resonances: δ 5.99 (s, 2 H, H⁵), 4.63 (br s, 8 H, =CH, COD). ¹H NMR (toluene-*d*₈, 300.12 MHz, -60 °C): δ 5.88 (br s, 1 H, =CH, COD), 5.75 (s, 1 H, H⁵), 5.62 (s, 1 H, H⁵), 5.58 (br s, 1 H, =CH, COD), 5.40 (br s, 1 H, =CH, COD), 4.74 (br s, 1 H, =CH, COD), 4.23 (br s, 1 H, =CH, COD), 4.11 (br s, 1 H, =CH, COD), 3.60 (br s, 1 H, =CH, COD), 3.40 (br s, 1 H, =CH, COD), 2.92 (br s, 5 H, N-CH₃ and CH₂, COD), 2.72 (br s, 1 H, CH₂, COD), 2.54 (s, 3 H, N-CH₃), 2.44 (br m, 5 H, CH₂, COD), 1.89 (br m, 2 H, CH₂, COD), 1.64 (br s, 9 H, CH₃, ^tBu), 1.32 (br s, 15 H, CH₂, COD and CH₃, ^tBu). ¹H NMR (CDCl₃, 400.16 MHz, 25 °C), selected resonances: δ 6.42 (s, 2 H, H⁵), 4.47 (br s, 8 H, =CH, COD), 3.42 (s, 6 H, N-CH₃). ¹H NMR (CDCl₃, 300.12 MHz, -55 °C): δ 6.47 (s, 1 H, H⁵), 6.42 (s, 1 H, H⁵), 4.82 (br m, 2 H, =CH, COD), 4.68 (br m, 1 H, =CH, COD), 4.13 (br m, 2 H, =CH, COD), 3.51 (br m, 1 H, =CH, COD), 3.40 (s, 3 H, N-CH₃), 3.37 (s, 3 H, N-CH₃), 3.12 (br s, 1 H, =CH, COD), 3.04 (br m, 1 H, =CH, COD), 2.48 (br m, 2 H, CH₂, COD), 2.31 (br m, 2 H, CH₂, COD), 2.01 (br m, 4 H, CH₂, COD), 1.86 (br m, 4 H, CH₂, COD), 1.75 (br s, 10 H, CH₂, COD and CH₃, ^tBu), 1.14 (br s, 13 H, CH₂, COD and CH₃, ^tBu). MS [FAB⁺ m/z (%): 939 (73) [M]⁺, 830 (9) [M⁺ - COD]. Anal. Calcd for C₃₂H₅₀N₄S₂Ir₂ (939.33): C, 40.92; H, 5.37; N, 5.96; S, 6.83. Found: C, 40.81; H, 4.98; N, 5.90; S, 6.81.

Synthesis of [Rh(μ-^tBu₂-ImS)(COD)]₂ (13). Following the general procedure, [Rh(μ-OMe)(COD)]₂ (0.116 g, 0.239 mmol) and 1,4-di-*tert*-butylimidazole-2-thiol (0.102 g, 0.479 mmol) were used to prepare **13** (0.169 g, 84%). Two main species are observed by NMR at RT in CD₂Cl₂: A (dinuclear) and B (mononuclear), in a ratio of 85% to 15%. ¹H NMR (CD₂Cl₂, 400.16 MHz, 25 °C), selected resonances: δ 6.61 (br s, 2 H, H⁵, A), 6.21 (s, 1 H, H⁵, B), 4.00–4.56 (br m, 8 H, =CH, COD, A), 1.56 (s, 9 H, N-^tBu, B), 1.08 (s, 9 H, ^tBu, B). ¹H NMR (toluene-*d*₈, 300.13 MHz, -60 °C): δ 6.63 (br m, 2 H, H⁵), 5.70 (br s, 4 H, =CH, COD), 4.42 (br s, 4 H, =CH, COD), 3.71 (br s, 3 H, CH₂, COD), 2.94 (br s, 3 H, CH₂, COD), 2.24 (br m, 5 H, CH₂, COD), 1.80 (br m, 5 H, CH₂, COD), 1.54 (br s, 18 H, CH₃, N-^tBu), 1.37 (br s, 18 H, CH₃, ^tBu). MW: found 508 (calcd 844.8). MS [FAB⁺ m/z (%): 844 (11) [M]⁺, 736 (47) [M⁺ - COD], 633 (63) [M⁺ - ^tBu₂-ImS], 422 (100) [M⁺ - Rh(^tBu₂-ImS)(COD)]. Anal. Calcd for C₃₈H₆₂N₄S₂-Rh₂ (844.86): C, 54.02; H, 7.40; N, 6.63; S, 7.59. Found: C, 53.94; H, 7.00; N, 6.38; S, 7.41.

Synthesis of [Ir(μ-^tBu₂-ImS)(COD)]₂ (14). Following the general procedure, [Ir(μ-OMe)(COD)]₂ (0.175 g, 0.264 mmol) and 1,4-di-*tert*-butylimidazole-2-thiol (0.112 g, 0.528 mmol) were used to prepare **14** (0.249 g, 92%). ¹H NMR (CD₂Cl₂, 400.16 MHz, 25 °C), selected resonances: δ 6.67 (s, unidentified isomer), 6.61 (s,

100.63 MHz, 25 °C): δ 190.2 (ddd, $^1J_{C-Rh} = 75.3$ Hz, $^2J_{C-P} = 17.1$ Hz, $^4J_{C-P}$ or $^3J_{C-Rh} = 2.9$ Hz, CO), 168.8 (SC), 168.4 (SC), 164.2 (C⁶), 162.1 (C⁶), 135.9 (d, $J_{C-P} = 44.6$ Hz, C_{ipso-P}), 135.5 (C³), 135.3 (d, $J_{C-P} = 12.4$ Hz, *o*-CH_{Ph}, PPh₃), 135.1 (C³), 130.1 (*p*-CH_{Ph}, PPh₃), 128.5 (d, $J_{C-P} = 10.24$ Hz, *m*-CH_{Ph}, PPh₃), 127.5 (C⁴), 125.0 (C⁴), 116.4 (C⁵), 115.6 (C⁵), 38.2 (C, 'Bu), 38.0 (C, 'Bu), 30.8 (CH₃, 'Bu). IR (toluene, cm⁻¹): 1989 (s), 1976 (m). MS [FAB⁺ *m/z* (%): 1120 (8) [MH]⁺, 1091 (11) [M⁺ - CO], 800 (69) [M⁺ - PPh₃ - 2CO]. Anal. Calcd for C₅₆H₅₄N₂O₂P₂S₂Rh₂ (1118.92): C, 60.11; H, 4.86; N, 2.50; S, 5.73. Found: C, 60.01; H, 4.56; N, 2.47; S, 5.61.

Synthesis of [Ir(μ -⁴Bu-PyS)(CO)(PPh₃)₂] (6). [Ir(acac)(CO)(PPh₃)₂] (0.174 g, 0.300 mmol) and 6-*tert*-butylpyridine-2-thiol (0.0501 g, 0.300 mmol) were dissolved in dry CH₂Cl₂ (2 mL) to obtain a red solution. The reaction mixture was stirred 0.5 h at room temperature and concentrated to 1 mL. The reaction mixture was cooled in an ¹PrOH/CO₂ bath, and cold MeOH (3 mL) was added to obtain a gummy product. The solvent was removed under vacuum and the residue dissolved in CH₂Cl₂ (1 mL). Hexane was added, but no precipitate was observed. The solvent was removed under vacuum and the residue dissolved in CH₂Cl₂ (1 mL). Diethyl ether (3 mL) was added and an orange solid precipitated. Filtration and washing with cold diethyl ether (2 \times 2 mL) followed by drying under vacuum gave product (0.144 g, 74%). This compound is not stable in solution and is air sensitive. ¹H NMR (C₆D₆, 400.16 MHz, 25 °C): δ 8.04 (d, $J = 7.5$ Hz, 1H, H³), 7.90–7.94 (m, 1H, H³), 7.82–7.85 (m, 12H, *o*-CH_{Ph}, PPh₃), 7.19 (d, $J = 7.6$ Hz, 1H, H⁴), 6.96–7.00 (m, 18H, *p*-CH_{Ph} and *m*-CH_{Ph} of PPh₃), 6.82 (t, $J = 7.8$ Hz, 1H, H⁴), 6.71 (d, $J = 7.6$ Hz, 1H, H⁵), 6.66 (d, $J = 7.8$ Hz, 1H, H⁵), 1.41 (s, 9H, CH₃, 'Bu), 1.26 (s, 9H, CH₃, 'Bu). ³¹P{¹H} NMR (C₆D₆, 161.99 MHz, 25 °C): δ 20.5. MS [FAB⁺ *m/z* (%): 1298 (68) [MH]⁺, 1038 (30) [M⁺ - PPh₃], 1008 (32) [M⁺ - PPh₃ - CO]. Anal. Calcd for C₅₆H₅₄N₂O₂P₂S₂Ir₂ (1297.55): C, 51.84; H, 4.19; N, 2.16; S, 4.94. Found: C, 51.51; H, 4.08; N, 1.99; S, 4.90.

Synthesis of [Rh(μ -Me-⁴Bu-ImS)(CO)(PPh₃)₂] (11). [Rh(acac)(CO)(PPh₃)₂] (0.200 g, 0.406 mmol) and 1-methyl-4-*tert*-butylimidazole-2-thiol (0.0691 g, 0.406 mmol) were dissolved in dry CH₂Cl₂ (4 mL) to obtain a red solution. The reaction mixture was stirred 1 h at room temperature and concentrated to 1 mL. Cold MeOH (5 mL) was added and the mixture concentrated until an orange solid precipitated. The mixture was cooled in an ¹PrOH/CO₂ bath, leading to further precipitation. The orange solid was filtered using a cannula, washed with cold MeOH (2 \times 2 mL), and vacuum-dried (0.179 g, 78%). ¹H NMR (toluene-*d*₈, 300.12 MHz, 25 °C): δ 7.90 (br m, CH_{Ph}, PPh₃), 7.70 (m, CH_{Ph}, PPh₃), 7.03 (br m, CH_{Ph}, PPh₃), 5.64 (s, 2 H, H⁵), 2.73 (s, 6 H, N-CH₃), 1.37 (s, 18 H, CH₃, 'Bu). ¹H NMR (toluene-*d*₈, 300.12 MHz, -60 °C): δ 8.94 (br m, CH_{Ph}, PPh₃), 8.00 (br m, CH_{Ph}, PPh₃), 7.82 (br m, CH_{Ph}, PPh₃), 7.69 (m, CH_{Ph}, PPh₃), 7.36 (br m, CH_{Ph}, PPh₃), 7.11 (br m, CH_{Ph}, PPh₃), 6.94 (br m, CH_{Ph}, PPh₃), 6.84 (br m, CH_{Ph}, PPh₃), 6.67 (br m, CH_{Ph}, PPh₃), 5.51 (s, 2 H, H⁵), 2.63 (s, 6 H, NCH₃), 1.41 (br s, 18 H, CH₃, 'Bu). ³¹P{¹H} NMR (toluene-*d*₈, 121.49 MHz, 25 °C): δ 40.6 (d, $J_{P-Rh} = 165.0$ Hz, minor isomer), 38.7 (d, $J_{P-Rh} = 161.4$ Hz). ³¹P{¹H} NMR (toluene-*d*₈, 121.49 MHz, -60 °C): δ 49.9 (d, $J_{P-Rh} = 163.7$ Hz, minor isomer), 39.2 (d, $J_{P-Rh} = 160.1$ Hz). IR (cyclohexane, cm⁻¹): 1974 (s). MS [FAB⁺ *m/z* (%): 1125 (10) [M⁺], 1096 (46) [M⁺ - CO], 955 (35) [M⁺ - Me-⁴Bu-ImS]. Anal. Calcd for C₅₄H₅₆N₄O₂P₂S₂ (1124.93): C, 57.65; H, 5.02; N, 4.98; S, 5.70. Found: C, 57.33; H, 4.98; N, 4.93; S, 5.30.

Synthesis of [Ir(μ -Me-⁴Bu-ImS)(CO)(PPh₃)₂] (12). [Ir(acac)(CO)(PPh₃)₂] (0.1152 g, 0.198 mmol) and 1-methyl-4-*tert*-butylimidazole-2-thiol (0.0337 g, 0.198 mmol) were dissolved in dry CH₂Cl₂ (2 mL) to obtain a red solution. The reaction mixture was stirred 0.5 h at room temperature and concentrated to 1 mL. Diethyl ether (3 mL) was added and the mixture concentrated until orange

solid precipitated. The mixture was cooled in an ¹PrOH/CO₂ bath, and additional cold diethyl ether (2 mL) was added. The orange solid was filtered with a cannula, washed with cold diethyl ether (3 \times 2 mL), and vacuum-dried (0.153 g, 68%). This compound is not stable in solution and is air sensitive. ¹H NMR (C₆D₆, 400.16 MHz, 25 °C): δ 7.93 (br s, CH_{Ph}, PPh₃), 7.81 (m, CH_{Ph}, PPh₃), 7.00 (br m, CH_{Ph}, PPh₃), 5.54 (s, 2 H, H⁵), 2.66 (s, 6 H, N-CH₃), 1.41 (s, 18 H, CH₃, 'Bu). ¹H NMR (toluene-*d*₈, 300.12 MHz, -60 °C): δ 8.95 (m, CH_{Ph}, PPh₃), 8.03 (m, CH_{Ph}, PPh₃), 7.77 (m, CH_{Ph}, PPh₃), 7.42 (m, CH_{Ph}, PPh₃), 7.15 (br m, CH_{Ph}, PPh₃), 7.07 (br m, CH_{Ph}, PPh₃), 6.98 (br m, CH_{Ph}, PPh₃), 6.82 (m, CH_{Ph}, PPh₃), 6.66 (m, CH_{Ph}, PPh₃), 5.33 (s, 2 H, H⁵), 2.54 (s, 6 H, N-CH₃), 1.43 (br s, CH₃, 'Bu). ³¹P{¹H} NMR (C₆D₆, 121.49 MHz, 25 °C): δ 22.25, 17.95 (second isomer). ³¹P{¹H} NMR (toluene-*d*₈, 121.49 MHz, -60 °C): δ 22.13. IR (cyclohexane, cm⁻¹): 1973 (s). MS [FAB⁺ *m/z* (%): 1303 (7) [M⁺], 1042 (20) [M⁺ - PPh₃], 984 (9) [M⁺ - PPh₃ - 2CO]. Anal. Calcd for C₅₄H₅₆N₄O₂P₂S₂Ir₂ (1303.55): C, 49.75; H, 4.33; N, 4.30; S, 4.92. Found: C, 49.63; H, 4.15; N, 4.40; S, 4.81.

Synthesis of [Rh(μ -⁴Bu₂-ImS)(CO)(PPh₃)₂] (17). Carbon monoxide was bubbled through an orange solution of complex **13** (0.101 g, 0.120 mmol) in CH₂Cl₂ (10 mL) for 10 min, and the solution color changed to red. Solid triphenylphosphine (0.063 g, 0.240 mmol) was then added to give a yellow solution with evolution of carbon monoxide. The reaction mixture was stirred for 1 h at room temperature. Workup as described in the synthesis of compound **5** gave the complex as a yellow solid (0.106 g, 73%). ¹H NMR (C₆D₆, 400.16 MHz, 25 °C): δ 7.83–7.85 (m, 6 H, *o*-CH_{Ph}, PPh₃), 6.98–7.02 (m, 9 H, *p*-CH_{Ph} and *m*-CH_{Ph} of PPh₃), 6.20 (s, 1 H, H⁵), 1.47 (s, 9 H, CH₃, N-⁴Bu), 1.25 (s, 9 H, CH₃, 'Bu). ³¹P{¹H} NMR (toluene-*d*₈, 121.49 MHz, 25 °C): δ 49.83 (br d, $J_{P-Rh} = 156.3$ Hz). ³¹P{¹H} NMR (toluene-*d*₈, 121.49 MHz, -60 °C): δ 49.84 (d, $J_{P-Rh} = 162.0$ Hz). ¹³C{¹H} APT NMR (C₆D₆, 100.63 MHz, 25 °C): δ 189.8 (dd, $J_{C-Rh} = 75.3$ Hz, $J_{C-P} = 19.7$ Hz, CO), 157.9 (SC), 146.1 (C⁴), 135.2 (d, $J_{C-P} = 49.7$ Hz, C_{ipso-P}), 134.9 (d, $J_{C-P} = 11.7$ Hz, *o*-CH_{Ph}, PPh₃), 130.5 (d, $J_{C-P} = 2.1$ Hz, *p*-CH_{Ph}, PPh₃), 128.7 (d, $J_{C-P} = 10.2$ Hz, *m*-CH_{Ph}, PPh₃), 107.2 (C⁵), 56.4 (C, N-⁴Bu), 32.0 (C, 'Bu), 30.5 (CH₃, N-⁴Bu), 29.5 (CH₃, 'Bu). IR (CH₂Cl₂, cm⁻¹): 1968 (s). MW: found 605.8 (calcd 604.5). MS [FAB⁺ *m/z* (%): 605 (20) [MH]⁺, 577 (87) [M⁺ - CO]. Anal. Calcd for C₃₀H₃₄N₂O₂PSRh (604.54): C, 59.60; H, 5.67; N, 4.63; S, 5.30. Found: C, 59.72; H, 5.51; N, 4.45; S, 5.23.

Synthesis of [Ir(μ -⁴Bu₂-ImS)(CO)(PPh₃)₂] (18). Carbon monoxide was bubbled through a dark red solution of the complex [Ir(μ -⁴Bu₂-ImS)(COD)]₂ (**14**) (0.153 g, 0.150 mmol) in CH₂Cl₂ (8 mL) for 15 min, and the solution color changed to dark purple. Solid triphenylphosphine (0.063 g, 0.240 mmol) was then added and the mixture stirred for 0.5 h at room temperature under slight negative pressure to give an orange-yellow solution. Workup as described in the synthesis of compound **5** gave the complex as a yellow solid (0.135 g, 65%). ¹H NMR (C₆D₆, 400.16 MHz, 25 °C): δ 7.87–7.92 (m, 6 H, *o*-CH_{Ph}, PPh₃), 6.97–7.04 (m, 9 H, *p*-CH_{Ph} and *m*-CH_{Ph} of PPh₃), 5.98 (s, 1 H, H⁵), 1.46 (s, 9 H, CH₃, N-⁴Bu), 1.14 (s, 9 H, CH₃, 'Bu). ³¹P{¹H} NMR (C₆D₆, 161.99 MHz, 25 °C): δ 19.9. ¹³C{¹H} APT NMR (C₆D₆, 100.63 MHz, 25 °C): δ 176.6 (CO), 158.1 (SC), 145.6 (C⁴), 134.9 (d, $J_{C-P} = 10.9$ Hz, *o*-CH_{Ph}, PPh₃), 134.4 (presumably the upfield peak of a doublet for C_{ipso-P} , with the downfield peak obscured by the larger doublet centered at 134.9), 130.6 (d, $J_{C-P} = 2.1$ Hz, *p*-CH_{Ph}, PPh₃), 128.6 (d, $J_{C-P} = 10.2$ Hz, *m*-CH_{Ph}, PPh₃), 107.5 (C⁵), 56.4 (C, N-⁴Bu), 32.1 (C, 'Bu), 30.3 (CH₃, N-⁴Bu), 29.5 (CH₃, 'Bu). IR (CH₂Cl₂, cm⁻¹): 1953 (s). MW: found 648.1 (calcd 693.8). MS [FAB⁺ *m/z* (%): 694 (100) [M⁺]. Anal. Calcd for C₃₀H₃₄N₂O₂PIrS (693.85): C, 51.93; H, 4.94; N, 4.04; S, 4.62. Found: C, 51.62; H, 4.99; N, 3.97; S, 4.40.

Crystal Structure Determination of Complexes 2, 5, 7, 13, and 18. X-ray data were collected for all complexes at low

temperature [223(2) K for **2**, 173(2) K for **5**, and 100(2) K for **7**, **13**, and **18**] on a Bruker SMART APEX CCD diffractometer with graphite-monochromated Mo K α radiation ($\lambda = 0.71073 \text{ \AA}$). Data were corrected for absorption using a multiscan method applied with the SADABS program.⁵² The structures were solved by direct methods with SHELXS-86.⁵³ Refinement, by full-matrix least squares on F^2 with SHELXL97,⁵³ was similar for all complexes, including isotropic and subsequently anisotropic displacement parameters for all non-hydrogen nondisordered atoms. Particular details concerning the existence of static disorder and hydrogen refinement are listed below. All the highest electronic residuals were observed in close proximity to the metals (or in the disorder region) and have no chemical sense.

Refinement details for **2**: One of the *tert*-butyl substituents was observed disordered, and a model with two complementary positions was included. Hydrogens were included in calculated positions, and riding refinement was used. Details for **5**: One ^tBu substituent exhibited high thermal parameters; no clear model of disorder could be established; eventually dynamic disorder was assumed. Hydro-

gens, except those of the ^tBu moiety, were included from observed positions and refined as isotropic atoms. Details for **7**: Two independent, but chemically analogous, molecules were observed in the crystal structure. High thermal parameters revealed the existence of static disorder in three different spatial regions: two ^tBu groups and part of a cyclooctadiene molecule [atoms C(12)–C(15)]; a model based on two moieties was used in each case. Hydrogens were included in calculated positions for all nondisordered atoms; riding refinement was used. Details for **13**: A methanol solvent molecule was present in the crystal structure. Hydrogens were in calculated positions; riding model was used. Refinement for **18**: Hydrogens were included in observed positions; refinement was performed as free isotropic atoms.

Acknowledgment. The financial support of Consejo Nacional de Ciencia y Tecnología (CONACyT, Mexico) (grant 38829-E), Ministerio de Ciencia y Tecnología (MCyT, Spain) (grant BQU2002-1729), a graduate scholarship (CONACyT) for V.M.S., and Fundación Carolina (support for V.M.S.) are acknowledged.

Supporting Information Available: CIF files for all crystal structures. This information is available free of charge via the Internet at <http://pubs.acs.org>.

OM060317T

(52) SAINT+ Software for CCD diffractometers; Bruker AXS: Madison, WI, 2000. Sheldrick, G. M. *SADABS, Program for Correction of Area Detector Data*; University of Göttingen: Göttingen, Germany, 1999.

(53) SHELXTL Package v. 6.10; Bruker AXS: Madison, WI, 2000. Sheldrick, G. M. *SHELXS-86* and *SHELXL-97*; University of Göttingen: Göttingen, Germany, 1997.